Redshift distances in flat Friedmann-Lemaître-Robertson-Walker spacetime

Steffen Haase[*1]

[*]Leipzig, Germany

Abstract

In the present paper we use the flat Friedmann-Lemaître-Robertson-Walker metric describing a spatially homogeneous and isotropic universe to derive the cosmological redshift distance in a way which differs from that which can be found in the astrophysical literature.

We use the co-moving coordinate r_e (the subscript **e** indicates **e**mission) for the place of a galaxy which is emitting photons and r_a (the subscript **a** indicates **a**bsorption) for the place of an observer within a different galaxy on which the photons - which were traveling thru the universe - are absorbed. Therefore the real physical distance - the way of light - is calculated by $D = a(t_0)\, r_a - a(t_e)\, r_e$. Here means $a(t_0)$ the today's (t_0) scale parameter and $a(t_e)$ the scale parameter at the time of emission (t_e) of the photons. Nobody can doubt this real travel way of light: The photons are emitted on the co-moving coordinate place r_e and are than traveling to the co-moving coordinate place r_a. During this traveling the time is moving from t_e to t_0 ($t_e \leq t_0$) and therefore the scale parameter is changing in the meantime from $a(t_e)$ to $a(t_0)$.

Using this right way of light we calculate some relevant classical cosmological equations (effects) and compare these theoretical results with some measurements of astrophysics (quasars, SNIa and black hole in M87) to get the parameters of the theory.

We get the today's Hubble parameter $H_0 \approx 65.638$ km/(s Mpc) as a result. This value is smaller than the Hubble parameter $H_{0,Planck} \approx 67.66$ km/(s Mpc) resulting from Planck 2018 data which is discussed in the literature. Furthermore, we find for the radius of the Friedmann sphere $R_{0a} \approx 2{,}712.48$ Mpc. The today's mass density of the Friedmann sphere results in $\rho_0 \approx 4.843 \times 10^{-27}$ g/cm^3. For the mass of the Friedmann sphere we get $M_{FS} \approx 1.206 \times 10^{56}$ g. The mass of black hole within the galaxy M87 has the value $M_{BH,\,M87} \approx 2.358 \times 10^{45}$g.

Key words: relativistic astrophysics, theoretical and observational cosmology, redshift, Hubble parameter, quasar, galaxy, M87, SNIa, black hole

PACS NO:

[1] steffen_haase@vodafone.de

Contents:

List of Figures:

List of Tables:

"*Redshifts are the lifeblood of cosmology*."
E. M. Burbidge and G. Burbidge [11]

1. Introduction

The current cosmological standard model assumes the correctness of Einstein's field equations (EFE) containing the cosmological term Λ

$$G_{\mu\nu} = \frac{8\pi G}{c^4} T_{\mu\nu} - \Lambda g_{\mu\nu} \tag{1}$$

and solves these equations with the help of the Friedmann-Lemaître-Robertson-Walker metric (FLRWM)

$$ds^2 = c^2 dt^2 - a^2(t)\left[\frac{dr^2}{1-\varepsilon r^2} + r^2(d\vartheta^2 + \sin^2\vartheta d\varphi^2)\right] \quad , \tag{2}$$

which is suitable for the description of a homogeneous and isotropic universe evolving over time.

The solutions found by solving the EFE are the Friedmann equations (FE)

$$\left(\frac{\dot{a}}{a}\right)^2 = \frac{8\pi G}{3}\rho - \frac{\varepsilon c^2}{a^2} + \frac{\Lambda c^2}{3} \qquad \textit{and} \qquad \frac{\ddot{a}}{a} = -\frac{4\pi G}{3}\left(\rho + \frac{3P}{c^2}\right) + \frac{\Lambda c^2}{3} \quad . \tag{3}$$

$G_{\mu\nu}$ is the Einstein tensor, G the gravitational constant, $T_{\mu\nu}$ the energy-momentum tensor and Λ the cosmological constant that Einstein added to his original field equations, but later discarded. With ε = 0, +1 or -1 the constant of curvature was introduced and r, ϑ and φ are spherical polar coordinates. The time-dependent scale parameter was designated with a(t) and its time derivatives with points above. P is the pressure of matter and ρ is its density.

Both FE together lead to the law of conservation of energy

$$\frac{d}{dt}\left(a^3\rho c^2\right) + P\frac{d}{dt}a^3 = 0 \quad , \tag{4}$$

which for pressure less matter then turns into a law of conservation of mass because of P = 0:

$$\frac{d}{dt}\left(a^3\rho c^2\right)=0 \qquad or \qquad a^3\rho \propto M = const \qquad because\ of \qquad \rho \propto \frac{M}{a^3} \quad . \tag{5}$$

This mass M contains all matter that is gravitationally effective in the universe.
In practice, due to the existence of the conservation law, only the first of the two Friedmann equations (3) is usually used.

1.1 Simplifying assumptions

The application of the theoretical standard cosmology to the measured data of the observational cosmology shows that the universe is flat. For this reason, the curvature constant ε is negligible. We agree with this finding, whereby the FLRWM and the FE simplify to

$$ds^2 = c^2dt^2 - a^2(t)\left[dr^2 + r^2(d\vartheta^2 + \sin^2\vartheta d\varphi^2)\right] \tag{2a}$$

and

$$\left(\frac{\dot{a}}{a}\right)^2 = \frac{8\pi G}{3}\rho + \frac{\Lambda c^2}{3} \quad , \tag{3a}$$

respectively.

The standard cosmology uses the following density parameters $\Omega_{0,\,i}$ (i = M, R, Λ) for the different types of matter that may exist in the universe

$$\Omega_{0,M} = \frac{\rho_{0,M}}{\rho_{0,c}}, \qquad \Omega_{0,R} = \frac{\rho_{0,R}}{\rho_{0,c}}, \qquad \Omega_{0,\Lambda} = \frac{\rho_{0,\Lambda}}{\rho_{0,c}}$$
$$with \qquad \rho_{0,c} \equiv \frac{3H_0^{\,2}}{8\pi G} \approx 1{,}878\times10^{-29}\ h^2 g/cm^3 \tag{6}$$

and determines their values using measurement data from observing cosmology. With $\rho_{0,\,M}$ today's density (first index 0) of the non-relativistic matter was introduced and $\rho_{0,R}$ describes the today's density of the relativistic matter, e.g. radiation (index R). A today's density $\rho_{0,\Lambda}$ is assigned to the cosmological constant Λ and the today's so-called critical density is defined with $\rho_{0,\,c}$, which - neglecting the cosmological constant - corresponds to an equilibrium between kinetic energy ($da/dt \neq 0$) and potential energy of gravitation. H_0 is today's Hubble parameter. The dimensionless parameter h scales the Hubble parameter.

The evaluation of the measurement data using standard cosmology shows that today's quotient of $\rho_{0,r}/\rho_{0,m}$ being

$$\frac{\Omega_{0,R}}{\Omega_{0,M}} = \frac{\rho_{0,R}}{\rho_{0,M}} \approx \frac{8.5 \times 10^{-5}}{0.3} \approx 2.83 \times 10^{-4} \tag{6a}$$

is very small, which is why today's radiation density $\rho_{0,R}$ can be neglected compared to today's non-relativistic matter density $\rho_{0,M}$. We make use of this knowledge when deriving the redshift distance.

In the following, we also neglect the mathematical possible cosmological constant Λ. The comparison of the redshift distance derived here with measurement results shows in retrospect that this additional parameter is not required. As a result, the EFE are returned to their historically original form and the FE takes on the simpler form

$$\left(\frac{\dot{a}}{a}\right)^2 = \frac{8\pi G}{3}\rho \quad . \tag{3b}$$

2 Derivation of cosmological relevant relations

2.1 Previews

From the requirement of homogeneity it follows that all extra-galactic objects remain at their coordinate location r in the course of the temporal development of the universe, i.e. the coordinate distance between randomly selected galaxies does not change over time, the galaxies rest in this coordinate system. For this reason, dr/dt = 0 applies to them.
This does not apply to the freely moving photons in the universe: They detach themselves from a galaxy at a certain point in time at a certain coordinate location, and are then later absorbed at a completely different coordinate location. In addition, the time-dependent scale parameter a(t) changes between the two points in time which stretches all real physical distances if a cosmic expansion exists.

Here we introduce the designation $r_{\mathbf{e}}$ (the subscript **e** indicates **e**mission of light) for the coordinate location of the light-emitting galaxy and name the coordinate location of the galaxy in which the observer resides $r_{\mathbf{a}}$ (the subscript **a** indicates **a**bsorption of light). In the Euclidean space ($\varepsilon = 0$) considered here, both variables mark the coordinate distance from a coordinate origin r = 0. The constant coordinate distance between the two galaxies is therefore calculated to be $r_a - r_e$ if we assume that the galaxy of the observer is more depart from the coordinate origin as the light-emitting galaxy. The light should therefore move from the inside to the outside within a spherical assumed mass distribution (outgoing photons), which serves as a simple model for the universe (using the FLRWM, it is quite easy to arrange that all directions are of a radial kind).
Due to the measurable expansion of the universe we know that in the course of cosmic evolution all physical distances over the time-dependent scale parameter a(t) being stretched according to the FE (3b).
Then the conservation law for the product of the density of matter $\rho(t)$ and the cube of the scale parameter a(t)

$$\rho a^3 = A \tag{7}$$

also applies. This means that A is a constant which essentially corresponds to the mass of the visible part of the universe (here called the Friedmann sphere). Because of A = constant Eq. (7) can also be written as

$$A = \rho(t_0)\, a^3(t_0) = \rho(t_e)\, a^3(t_e) = \rho_0 a_0{}^3 = \rho_e a_e{}^3 \quad , \tag{8}$$

where ρ_e and ρ_0 denote the densities of the universe and a_e and a_0 are the scale parameters at two different times t_e (time point of **e**mission) and t_0 (today's time point of absorption), respectively. Using Eq. (7) the FE (3b) yields

$$\left(\frac{da}{dt}\right)^2 = \frac{8\pi G}{3}\frac{A}{a} = \frac{B}{a} \quad . \tag{9}$$

With B another constant was introduced which just summarizes other constants. Using the law of mass conservation (7) means also that the mass of the universe which is inside a Friedmann sphere with the current "radius" a(t) is responsible for the expansion. This applies to all points of time. "Radius" (in quoted marks) was written here because a(t) does not have the meaning of a real physical radius. Only the product of the co-moving radial coordinate r and the scale parameter a(t) has this significance, as we shall see immediately.

For a galaxy resting in the coordinate system of the FLRWM, the real physical distance from the coordinate origin becomes calculated to

$$R(t) = a(t)\int_0^r \frac{d\bar{r}}{\sqrt{1-\varepsilon\,\bar{r}^2}} = a(t)\, r \quad , \tag{10}$$

if $\varepsilon = 0$ is considered. The co-moving coordinate r does not depend on time for galaxies.

The physical distance of the light-emitting galaxy from the coordinate origin at time t_e is therefore

$$R_e(t_e) = a(t_e)\, r_e \equiv a_e r_e = R_{ee} \quad , \tag{11}$$

while for the analog distance of the galaxy containing the observer at the same time

$$R_a(t_e) = a(t_e)\, r_a \equiv a_e r_a = R_{ea} \tag{12}$$

applies. The physical distance of both galaxies at the time t_e is therefore

$$D(t_e) = D_e = a_e r_a - a_e r_e = a_e (r_a - r_e) \equiv D_e \quad . \tag{13}$$

For the distance between both cosmic objects at a later time - means today‘s time here - $t_0 > t_e$ then applies

$$D(t_0) = D_0 = a_0 r_a - a_0 r_e = a_0 (r_a - r_e) \equiv D_0 \quad . \tag{14}$$

However, both distances mentioned above are worthless for the computation of cosmological relevant relations, since the emitted photons make their way to the observer which has to be calculated in accordance with

$$D = a_0 r_a - a_e r_e \quad . \tag{15}$$

To see this, imagine a photon that detaches itself at the time $t_e < t_0$ from the emitting galaxy at the coordinate r_e, where the scale parameter at this time has the value a_e. After the photon has moved freely through the universe, it will arrive at the coordinate point r_a, the place of the observer within another galaxy, at time t_0, with the scale parameter at that time being a_0. Thus, the photon does not travel the path described by Eq. (13) nor by Eq. (14). The real distance traveled by the photon is always greater than any one of these distances. This must be taken into account when deriving the physical redshift distance.

The real physical light path is illustrated by the green line in Fig. 1:

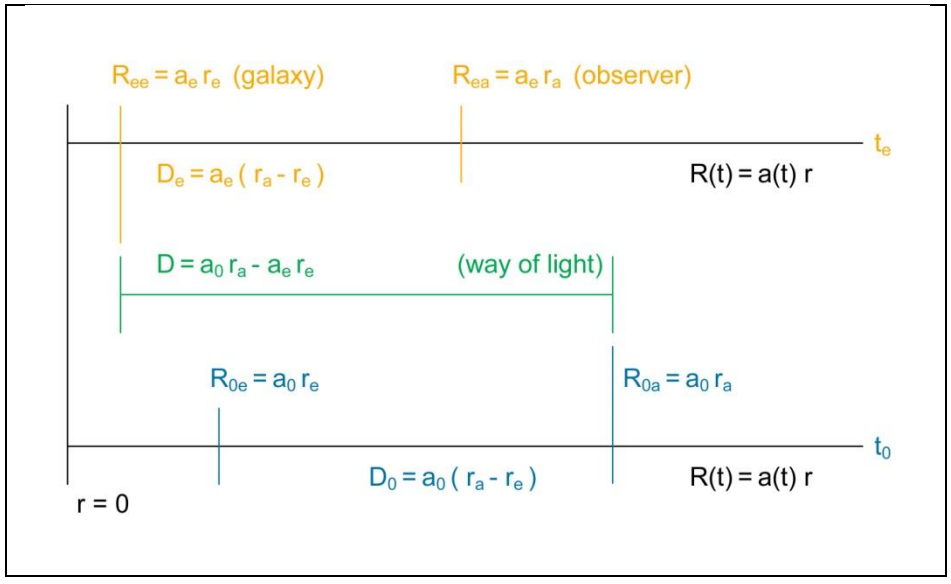

Figure 1. Real physical light path.

These remarks may be sufficient as a preliminary to the now following derivation of the redshift distance.

2.2 The redshift distance

We now want to investigate which equation results for the redshift distance (corresponding to the photon path), which depends on the redshift z, if the integral

$$\int_{r_e}^{r_a} dr = +\int_{t_e}^{t_0} \frac{c\,dt}{a(t)} \tag{16}$$

is used. This integral results for ε = 0 when the line element ds is set equal to zero in the FLRWM (2a) and radial (ϑ = φ = 0) outgoing photons are considered. Eq. (16) describes the motion of photons in the universe traveling from the coordinate r_e to the coordinate r_a.

During the travel time of the photons, the scale parameter changes from a_e to a_0. If the time differential is replaced using the FE (9), follows from Eq. (16)

$$\int_{r_e}^{r_a} dr = \frac{c}{\sqrt{B}} \int_{a_e}^{a_0} \frac{da}{\sqrt{a}} \quad . \tag{17}$$

After the execution of the integral we get

$$r_a - r_e = \frac{2c}{\sqrt{B}} \left(\sqrt{a_0} - \sqrt{a_e} \right) \quad . \tag{18}$$

Here we multiply both sides with a_0 and at the same time we extract the root of a_0 from the parenthesis:

$$a_0 r_a - a_0 r_e = \frac{2c}{\sqrt{B}} a_0^{3/2} \left(1 - \sqrt{\frac{a_e}{a_0}} \right) \quad . \tag{19}$$

On the left side of Eq. (19) is not yet the real path traveled by the photon, but the today's physical distance of the two galaxies involved.

We now introduce the redshift. To this end, we recall the simple relation between the scale parameters at two different times t_e and t_0 and the redshift z

$$\frac{a_0}{a_e} = 1 + z \qquad or \qquad \frac{a_e}{a_0} = \frac{1}{(1+z)} \tag{20a, b}$$

and also

$$a_0 = (1+z)a_e \quad . \tag{20c}$$

If Eq. (20b) is inserted into Eq. (19), the result is

$$a_0 r_a - a_0 r_e = \frac{2c}{\sqrt{B}} a_0^{3/2}\left(1 - \frac{1}{\sqrt{1+z}}\right) \quad . \tag{21}$$

Next, all unknown variables have to be eliminated from Eq. (21). First, we use the conservation law (8) in connection with Eq. (9) to eliminate a_0 on the right side of Eq. (21). The result is

$$a_0 r_a - a_0 r_e = \frac{2c}{\sqrt{\frac{8\pi G \rho_0}{3}}}\left(1 - \frac{1}{\sqrt{1+z}}\right) \quad , \tag{22}$$

where ρ_0 describes today's mass density of the universe.

For further derivation of the redshift distance, we now take into consideration the Eq. (20c)

$$a_0 r_a - (1+z)\, a_e r_e = \frac{2c}{\sqrt{\frac{8\pi G \rho_0}{3}}}\left(1 - \frac{1}{\sqrt{1+z}}\right) \tag{23}$$

to use then the light path D introduced by Eq. (15)

$$a_e r_e = a_0 r_a - D \tag{15a}$$

to get

$$a_0 r_a - (1+z)(a_0 r_a - D) = \frac{2c}{\sqrt{\frac{8\pi G \rho_0}{3}}}\left(1 - \frac{1}{\sqrt{1+z}}\right) \quad . \tag{24}$$

The further calculation results from suitable step-wise putting outside the brackets and summarization

$$a_0 r_a - (1+z)\, a_0 r_a + (1+z)\, D = \frac{2c}{\sqrt{\frac{8\pi G \rho_0}{3}}}\left(1 - \frac{1}{\sqrt{1+z}}\right) \tag{25}$$

and

$$-a_0 r_a z + (1+z) D = \frac{2c}{\sqrt{\frac{8\pi G \rho_0}{3}}} \left(1 - \frac{1}{\sqrt{1+z}} \right) \quad , \tag{26}$$

respectively.

$$(1+z) D = \frac{2c}{\sqrt{\frac{8\pi G \rho_0}{3}}} \left(1 - \frac{1}{\sqrt{1+z}} \right) + a_0 r_a z \quad . \tag{27}$$

Now we put $a_0 r_a$ outside the brackets on the right side of Eq. (27), which results in

$$(1+z) D = a_0 r_a \left[\frac{2c}{a_0 r_a \sqrt{\frac{8\pi G \rho_0}{3}}} \left(1 - \frac{1}{\sqrt{1+z}} \right) + z \right] \quad . \tag{28}$$

We introduce $R_{0a} = a_0 r_a$ as an abbreviation for the present physical location of the observer and solve Eq. (28) for D

$$D = \frac{R_{0a}}{(1+z)} \left[\frac{2c}{R_{0a} \sqrt{\frac{8\pi G \rho_0}{3}}} \left(1 - \frac{1}{\sqrt{1+z}} \right) + z \right] \quad . \tag{29}$$

As a further abbreviation we use

$$\frac{1}{\beta_0} = \frac{2c}{R_{0a} \sqrt{\frac{8\pi G \rho_0}{3}}} = \frac{c}{V_0} \tag{30}$$

resulting in

$$D(z; R_{0a}, \beta_0) = \frac{R_{0a}}{(1+z)} \left[\frac{1}{\beta_0} \left(1 - \frac{1}{\sqrt{1+z}} \right) + z \right] \quad . \tag{31}$$

The redshift distance D is therefore a function of z and the two parameters R_{0a} and β_0, which both can be determined by fitting the equation to the astrophysical measurements.

The name β_0 was chosen for the second parameter because it is a today's quotient of two velocities, where the denominator is the speed of light named c.

The literature does not know the parameter β_0. It results from the non-zeroing of r_a for the observer or of $r_e \neq 0$ for the observed galaxy.

For $\beta_0 = 1$, the simpler equation results

$$D(z; R_{0a}, \beta_0 = 1) = R_{0a}\left[1 - \frac{1}{(1+z)^{3/2}}\right] \quad . \tag{31a}$$

The expansion of Eq. (31) for small redshifts z leads to

$$D \approx \left(\frac{1}{2\beta_0} + 1\right) R_{0a} z \quad . \tag{32}$$

If this equation is solved for z and then multiplied by c, the result is

$$c\,z \approx \frac{c}{\left(\frac{1}{2\beta_0} + 1\right)} \frac{D}{R_{0a}} \quad . \tag{33}$$

That is how we find today's Hubble parameter

$$H_{0a} = \frac{c}{\left(\frac{1}{2\beta_0} + 1\right) R_{0a}} \quad . \tag{34}$$

The Hubble parameter also depends on the speed quotient β_0 introduced above and is in this form valid only for small redshifts because of the series expansion. This means that this H_{0a} is only valid locally.

For parameter $\beta_0 = 1$, we get

$$H_{0a} = \frac{2c}{3R_{0a}} \quad . \tag{34a}$$

The reciprocal of this is the Hubble time for $\beta_0 = 1$:

$$t_{H_{0a}} = \frac{3R_{0a}}{2c} \quad . \tag{34b}$$

We now give another expression for $1/\beta_0$

$$\frac{2c}{R_{0a}\sqrt{\frac{8\pi G\rho_0}{3}}} = 2\sqrt{\frac{R_{0a}}{R_S}} = \frac{1}{\beta_0} \quad , \tag{35}$$

which results from the Eq. (7) and Eq. (8)

$$M = \frac{4\pi}{3} A r_a^{\,3} = \frac{4\pi}{3} \rho_0 a_0^{\,3} r_a^{\,3} = \frac{4\pi}{3} \rho_0 R_{0a}^{\,3} \quad . \tag{36}$$

With $R_S = 2MG / c^2$, the Schwarzschild radius of mass M of the Friedmann sphere was introduced for pure formal reason. It does not play the same role here as it does within the Schwarzschild metric.

For $\beta_0 = 1/2$ we get $R_{0a} = R_S$. In this case we could believe that every observer is on the surface of a black hole (corresponds to the Friedmann sphere) and that he always looks into a black hole while observing. For a galaxy located in the center of the Friedmann sphere, an observer would measure an infinitely large redshift. Overall, that could be logical.

For $\beta_0 = 1$, $R_{0a} = R_S / 4$ would result and the speed V_0 would be exactly identical to the speed of light c.

The mass M contains all gravitational effective components of the visible universe: $M = \sum M_i$. These can also be different energy components E_i, to which, according to Einstein's energy-mass relationship $M_i = E_i/c^2$, masses M_i can be assigned. In addition, with M as the total mass, mass components that are invisible to us (perhaps only so far) are taken in to consideration.

With the help of Eq. (35) the Eq. (31) can be rewritten as

$$D(z; R_{0a}, R_S) = \frac{R_{0a}}{(1+z)}\left[2\sqrt{\frac{R_{0a}}{R_S}}\left(1 - \frac{1}{\sqrt{1+z}}\right) + z\right] \quad . \tag{31b}$$

If the comparison with the measurement data shows $\beta_0 = 1$, we would get

$$D(z;R_S)=\frac{R_S}{4}\frac{1}{(1+z)}\left[\left(1-\frac{1}{\sqrt{1+z}}\right)+z\right]$$

because of

$$\frac{1}{\beta_0}=1=2\sqrt{\frac{R_{0a}}{R_S}} \qquad or \qquad R_{0a}=\frac{R_S}{4} \quad .$$

This means

$$D(z;R_S)=\frac{R_S}{4}\left[1-\frac{1}{(1+z)\sqrt{1+z}}\right] \quad . \tag{31c}$$

In this case, we immediately see that the total mass M of the Friedmann sphere goes directly into the equation in the form of the formally introduced Schwarzschild radius R_S. Therefore, it can be used as a scale of cosmological distances.

Fig. 2 shows the redshift distance (31) normalized to the distance R_{0a} for various values of the parameter β_0.

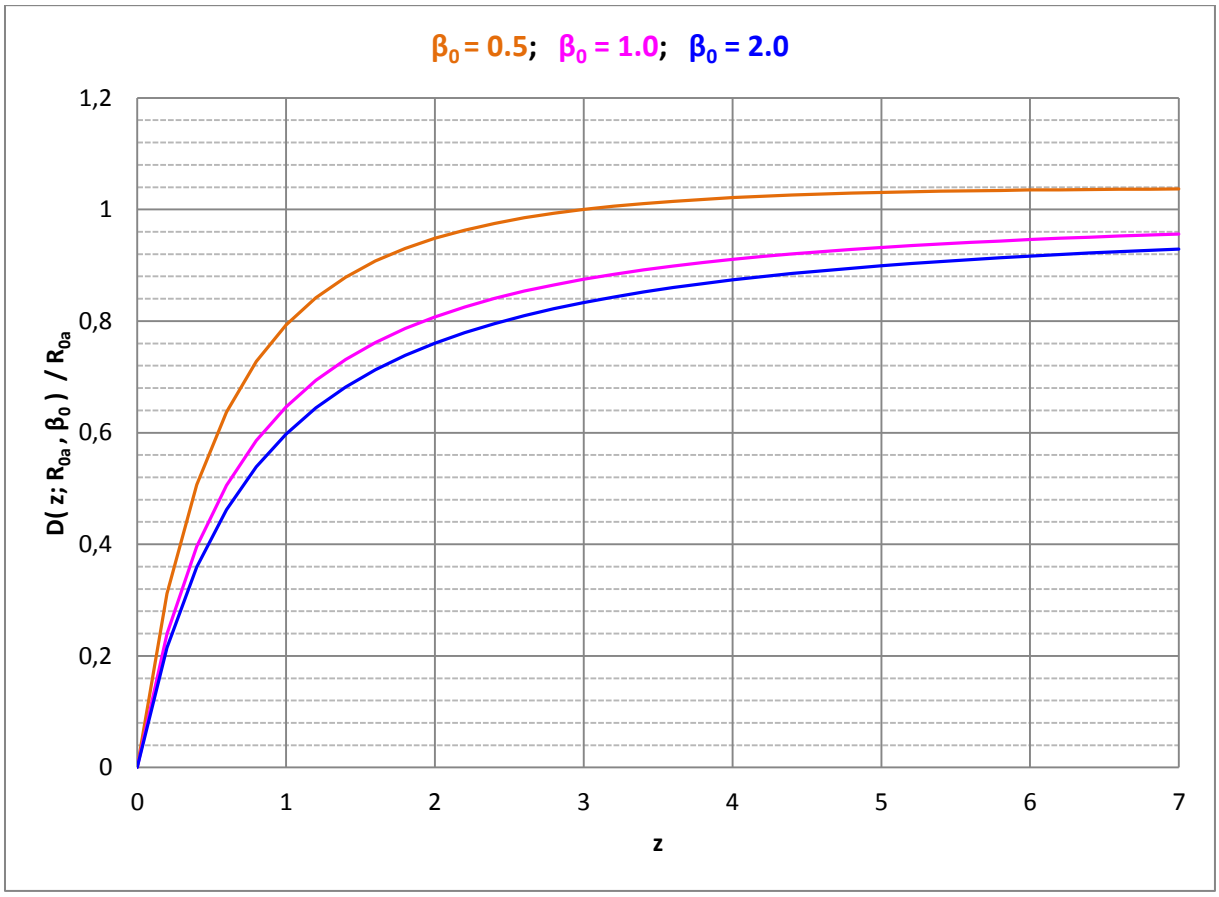

Figure 2. Redshift distance for different values of the parameter β_0.

The curvature of the curves is a direct consequence of the Friedmann equation.

For $\beta_0 = 1$, the distance $D = R_{0a}$ is achieved for $z = \infty$.

As a reminder: R_{0a} is today's distance of the observer from the origin of the coordinate system, who is placed on the surface of "his" Friedmann sphere.
The comparison of Eq. (31b) with a Hubble diagram thus determines the current radius $R_{0a} = a_0 r_a$ of the Friedmann sphere (today's physical location of the observer) and its Schwarzschild radius R_S.

Overall, each observer is located on the surface of all imaginable Friedmann spheres around him (for each viewing direction a Friedmann sphere with the radius R_{0a} belongs). The extragalactic objects (placed on $r = r_e$) observed by him then all lie according to their redshift z on a radial line somewhere between the observer (placed on $r = r_a$) and the center of the Friedmann sphere ($r = 0$).

The physical radius R_{0a} of the Friedmann sphere changes with time and forms a limit of visibility. Outside of every imaginable Friedmann sphere there is also mass, which, however, does not contribute to the gravitational events within the Friedmann sphere.

It should be mentioned that the conceivable Friedmann spheres naturally at least partially overlap.

An increasing limit distance R_{0a} decreases with time the velocity V_0 introduced above, because R_S is a constant. Because Eq. (31) describes the physical behavior of photons in the universe, the velocity V_0 in Eq. (30) could be interpreted as an effective speed of light c_{0*}

$$V_0 = \frac{R_{0a}}{2}\sqrt{\frac{8\pi G\rho_0}{3}} = \frac{c}{2}\sqrt{\frac{R_S}{R_{0a}}} \equiv c_{0*} \quad . \tag{30a}$$

This velocity changes according to R_{0a} and ρ_0, respectively, over the time and could have for us as today's observers just the value of the vacuum velocity c that we can measure today, if would be $\beta_0 = 1$.

If this possible interpretation is correct, the effective speed of light c_{0*} was infinitely large at the beginning of the expansion of the universe, because at that time the Friedmann sphere was infinitely small and respectively its matter density was infinitely large.

If we consider today's Hubble parameter (34) obtained above for small redshifts as a definition, we can write the redshift distance via

$$\frac{1}{\beta_0} = 2\left(\frac{c}{R_{0a}H_{0a}} - 1\right) \tag{34a}$$

also like this

$$D(z; R_{0a}, R_H) = \frac{R_{0a}}{(1+z)}\left[2\left(\frac{R_H}{R_{0a}} - 1\right)\left(1 - \frac{1}{\sqrt{1+z}}\right) + z\right] \quad . \tag{31d}$$

The quotient c/H_{0a} is called the Hubble radius R_H in the literature. For this distance, the escape speed by definition reaches the speed of light if it is assumed that a linear Hubble law is valid for all distances, which is - of course - not the case. The Eq. (31d) is therefore only valid for small redshifts how Eq. (34a).

2.3 The magnitude-redshift relation

The magnitude-redshift relation is given by the definition of the apparent magnitude m

$$m - m_{0a} = 5\log_{10}\frac{D}{R_{0a}} \quad . \tag{37}$$

Here an apparent limit magnitude m_{0a} was introduced for R_{0a}, which also changes with time. Substituting Eq. (31) into Eq. (37) then provides the sought magnitude-redshift relation

$$m(z; m_{0a}, \beta_0) = 5\log_{10}\left[\frac{1}{\beta_0}\left(1 - \frac{1}{\sqrt{1+z}}\right) + z\right] - 5\log_{10}(1+z) + m_{0a} \quad . \tag{38}$$

The two free parameters m_{0a} and β_0 can be determined by direct comparison with a magnitude-redshift diagram.

For $\beta_0 = 1$, the following simple equation results

$$m(z; m_{0a}) = 5\log_{10}\left[1 - \frac{1}{(1+z)^{3/2}}\right] + m_{0a} \quad . \tag{38a}$$

For comparison, reference is made here to Eq. (62) from chapter 5.2, which is known from the literature.

2.4 The angular size-redshift relation

This relation results in for large distances over

$$\varphi = \arcsin\frac{\delta}{D} \approx \frac{\delta}{D} \tag{39}$$

to

$$\varphi(z;\,\delta / D_{0a}, \beta_0) = \frac{\delta}{R_{0a}} \frac{(1+z)}{\left[\frac{1}{\beta_0}\left(1-\frac{1}{\sqrt{1+z}}\right)+z\right]} \quad . \tag{40}$$

In this equation φ means the measurable angular size and δ the linear size of the observed extra-galactic object.

Using $\beta_0 = 1$ we get

$$\varphi(z;\,\delta / R_{0a}) = \frac{\delta / R_{0a}}{\left[1-\frac{1}{(1+z)^{3/2}}\right]} \quad . \tag{40a}$$

In logarithmic form Eq. (40) becomes to

$$\log_{10}\varphi(z;\,\delta / R_{0a}, \beta_0) = \log_{10}\frac{\delta}{R_{0a}} - \log_{10}\left[\frac{1}{\beta_0}\left(1-\frac{1}{\sqrt{1+z}}\right)+z\right] + \log_{10}(1+z) \quad . \tag{41}$$

With $\beta_0 = 1$ we get the simplified equation

$$\log_{10}\varphi(z;\,\delta / R_{0a}) = \log_{10}\frac{\delta}{R_{0a}} - \log_{10}\left[1-\frac{1}{(1+z)^{3/2}}\right] \quad . \tag{41a}$$

For comparison, reference is made to Eq. (63) from chapter 5.2, which is known from the literature.

2.5 The number-redshift relation

In flat Euclidean space the equation for the light-path sphere becomes to

$$V = \frac{4\pi}{3} D^3 \quad . \tag{42}$$

If we introduce the redshift distance via Eq. (31)

$$V(z;\, R_{0a}, \beta_0) = \frac{4\pi}{3} \frac{{R_{0a}}^3}{(1+z)^3} \left[\frac{1}{\beta_0} \left(1 - \frac{1}{\sqrt{1+z}} \right) + z \right]^3 \tag{43}$$

we get for the number-redshift relation

$$N(z;\, N_{0a}, \beta_0) = \frac{N_{0a}}{(1+z)^3} \left[\frac{1}{\beta_0} \left(1 - \frac{1}{\sqrt{1+z}} \right) + z \right]^3 \quad , \tag{44}$$

where N_{0a} means the expected number of objects in the light-path sphere V_{0a} and besides

$$N_{0a} = V_{0a}\eta = \frac{4\pi}{3} {R_{0a}}^3 \eta \qquad and \qquad N = V\eta \tag{45a, b}$$

applies. With η the number density was named. In logarithmic form results

$$\log_{10} N(z;\, N_{0a}, \beta_0) = 3\log_{10} \left[\frac{1}{\beta_0} \left(1 - \frac{1}{\sqrt{1+z}} \right) + z \right] - 3\log_{10}(1+z) + \log_{10} N_{0a} \quad . \tag{46}$$

If we here also set $\beta_0 = 1$, we get

$$\log_{10} N(z;\, N_{0a}) = 3\log_{10} \left[1 - \frac{1}{(1+z)^{3/2}} \right] + \log_{10} N_{0a} \quad . \tag{46a}$$

For comparison, reference is made to Eq. (64) from chapter 5.2, which is known from the literature.

3. Derivation of further physical redshift distances

The starting point for the derivation of the further redshift distances are the elementary equations

$$(1+z) = \frac{a_0}{a_e} \qquad (20a) \qquad and \qquad D = R_{0a} - R_{ee} \qquad (15)$$
$$and \qquad (1+z) = \frac{a_0 r_a}{a_e r_a} = \frac{R_{0a}}{R_{ea}} \qquad and \qquad (1+z) = \frac{a_0 r_e}{a_e r_e} = \frac{R_{0e}}{R_{ee}} \quad . \tag{47}$$

This results in the following distances

$$R_{ee} = R_{0a} - D \qquad and \qquad R_{ea} = \frac{R_{0a}}{(1+z)}$$
$$and \qquad R_{0e} = (1+z)R_{ee} = (1+z)(R_{0a} - D) \quad . \tag{48}$$

R_{ee} is the then distance between the galaxy emitting the light and the origin of the coordinates - at the time t_e the light was emitted.

R_{ea} is the distance of the observer's galaxy from the origin of the coordinates at that time.

R_{0e} is the today's - at time t_0, at which the light is absorbed by the observer - distance of the light-emitting galaxy from the origin of the coordinates.

R_{0a} is today's distance of the galaxy containing the observer from the origin of the coordinates.

These distances become concretely with Eq. (31)

$$R_{ee}(z; R_{0a}, \beta_0) = R_{0a}\left\{1 - \frac{1}{(1+z)}\left[\frac{1}{\beta_0}\left(1 - \frac{1}{\sqrt{1+z}}\right) + z\right]\right\} \tag{49}$$

and

$$R_{0e}(z;\, R_{0a}, \beta_0) = R_{0a}\left[1 - \frac{1}{\beta_0}\left(1 - \frac{1}{\sqrt{1+z}}\right)\right] \tag{50}$$

and of course too

$$R_{ea}(z; R_{0a}) = \frac{R_{0a}}{(1+z)} \quad . \tag{51}$$

These distances from the coordinate origin result in

$$D_e(z;\, R_{0a}, \beta_0) = \frac{R_{0a}}{\beta_0}\frac{\left(1 - \frac{1}{\sqrt{1+z}}\right)}{(1+z)} \quad . \tag{52}$$

D_e is the then (t_e) distance between the observed galaxy and the galaxy in which the observer is located.

Furthermore we find

$$D_0(z; R_{0a}, \beta_0) = \frac{R_{0a}}{\beta_0}\left(1 - \frac{1}{\sqrt{1+z}}\right) \quad . \tag{52}$$

D_0 is the today's distance between the two participating galaxies.

The following figures illustrate the equations for the further redshift distances, where we have normalized all distances to R_{0a}.

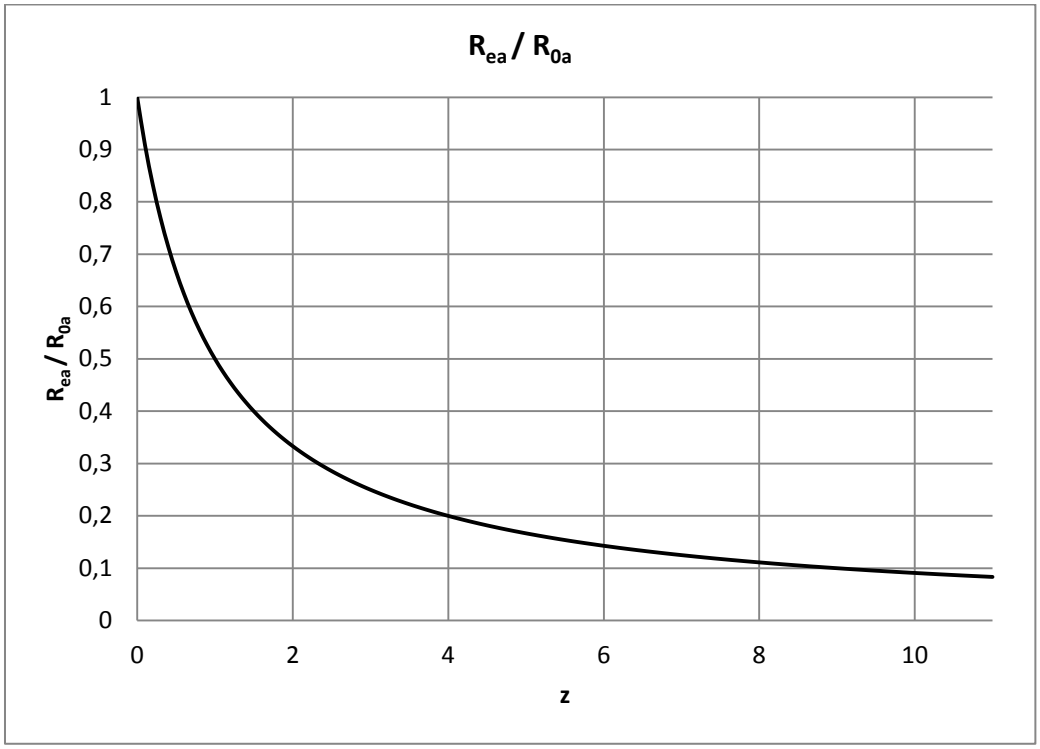

Figure 3. Redshift distance R_{ea} normalized to the distance R_{0a}.

This distance does not depend on the parameter β_0.

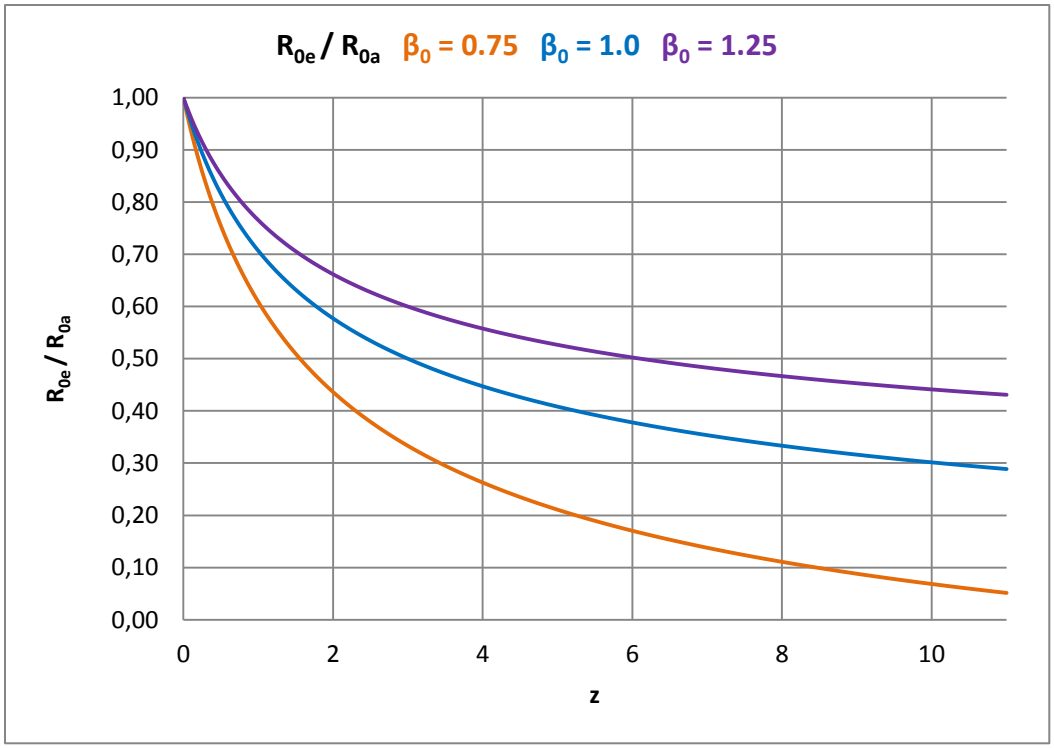

Figure 4. Redshift distance R_{0e} normalized to the distance R_{0a} for various values of the parameter β_0.

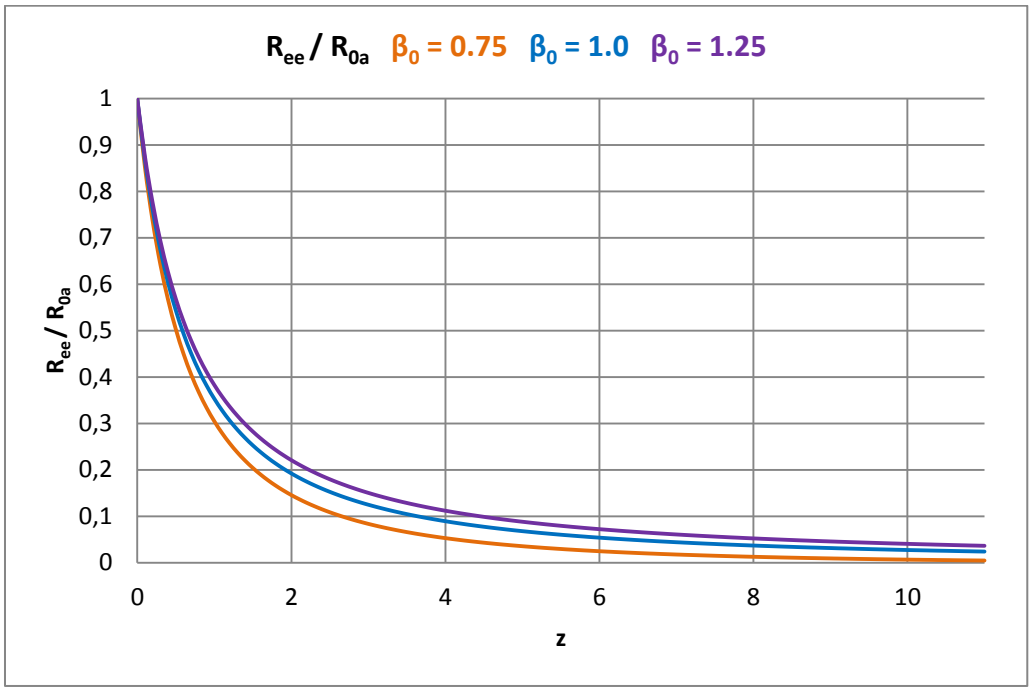

Figure 5. Redshift distance R_{ee} normalized to the distance R_{0a} for different values of the parameter β_0.

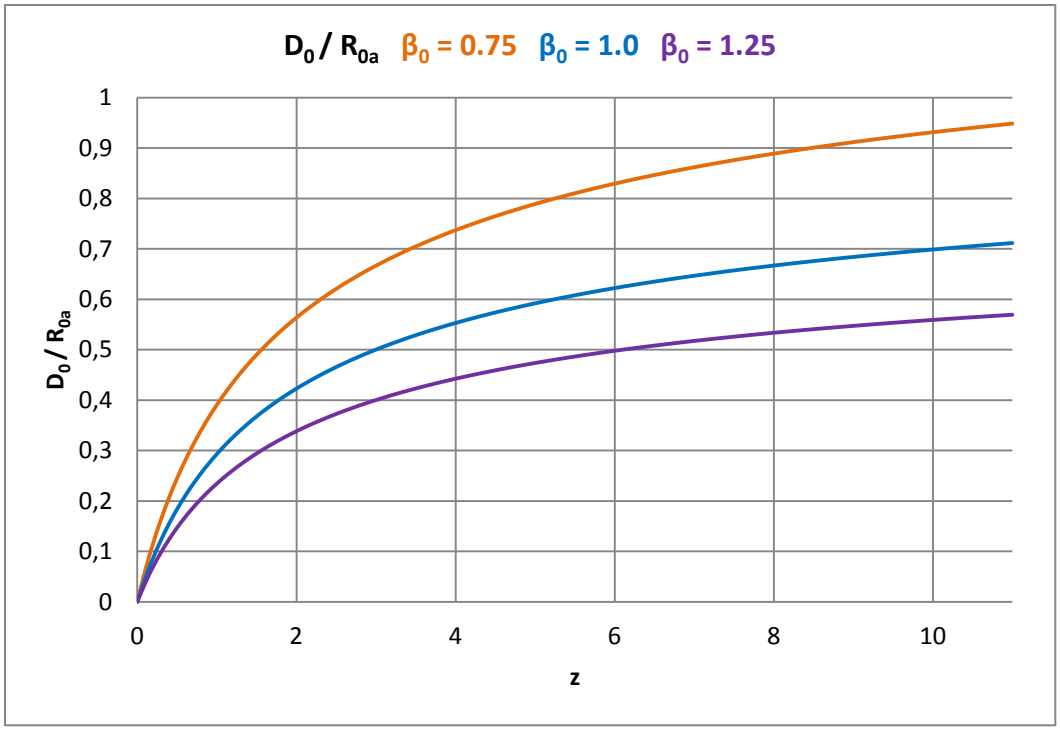

Figure 6. Today's (t_0) redshift distance D_0 normalized to the distance R_{0a} for various values of the parameter β_0.

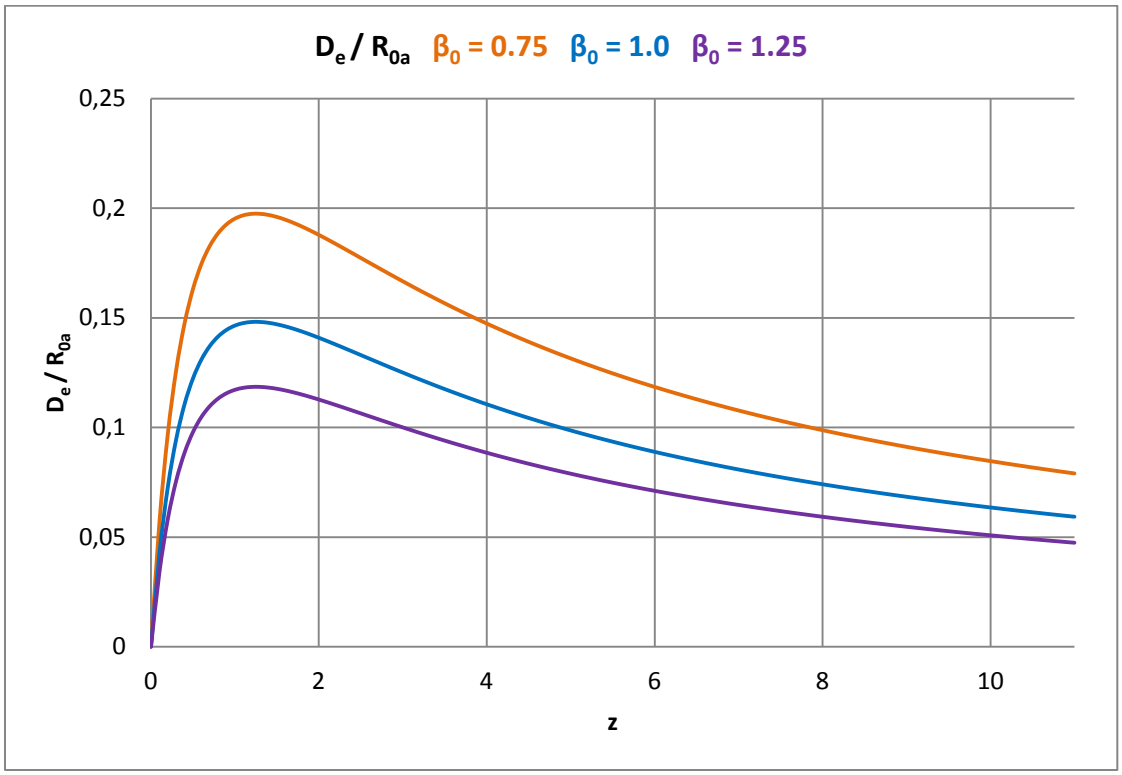

Figure 7. The at that time (t_e) redshift distance D_e normalized to the distance R_{0a} for various values of the parameter β_0.

In the specialist literature, none of these redshift distances are known and they cannot be derived there, respectively.

We will give concrete values for these redshift distances for the galaxy M87 and 27 SNIa below.

4. Determination of the parameter values

The present paper presents a theoretical derivation of redshift distances, which is done without approximations for e.g. small redshifts z and is, therefore, mainly of theoretical nature. The essay is therefore a theoretical offer to the observing cosmologists.

Nevertheless, in this chapter, we will apply the theory presented here in detail to some measurement results of observational cosmology, whereby we only demonstrate the principle of evaluating the measurement data. For this reason, no more detailed error analyzes are carried out. We leave that to the experts of observational cosmology.

4.1 Magnitude-redshift relation

The apparent magnitude m depends according to Eq. (38) in addition to the measurable redshift z also on the parameters β_0 and m_{0a}.

To find both parameters, the quasar catalog by Véron-Cetty [1] is suitable in which measured redshifts and apparent magnitudes of 132,975 quasars are given.
Fig. 8 shows all these quasars in a single magnitude-redshift diagram, where we have used $\log_{10}(cz)$ as the axis of ordinate.

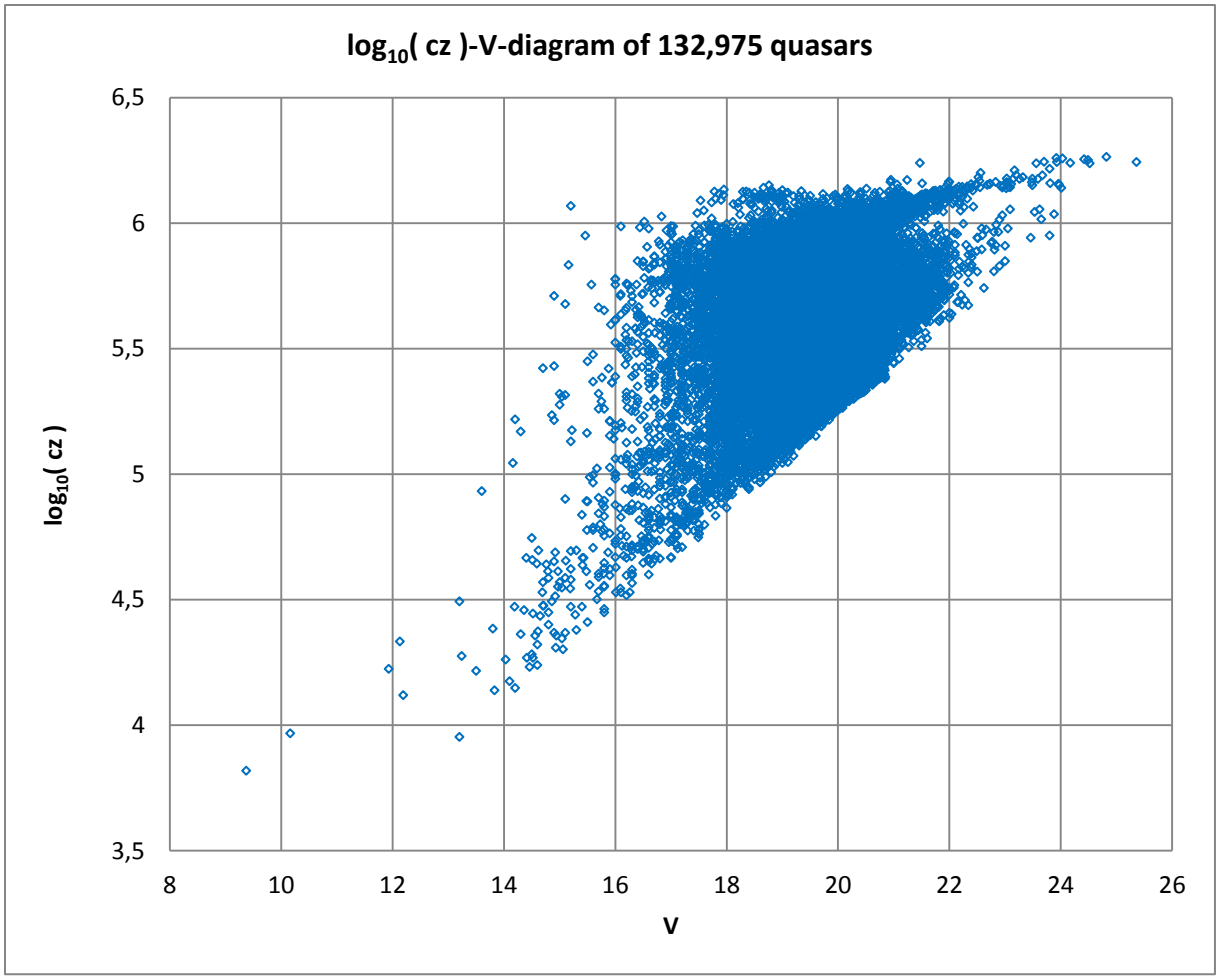

Figure 8. Magnitude-redshift diagram for all 132,975 quasars according to M.-P. Véron-Cetty et al. [1].

A clear edge can be seen on the right side of the accumulation of measurement points, which indicates minimum apparent magnitudes for associated redshifts. The apparent magnitudes are usually up to far to the left of this edge in the diagram.

If we form redshift intervals with mean values of the redshifts and the corresponding mean values for the apparent magnitude, this fact leads to a clear curvature of the mean value curve in the direction of the redshift axis.

The quasars therefore cannot be described in the diagram by a linear curve. This suggests that our redshift distance [i.e. ultimately Eq. (38)] could be suitable for the measured values.

It is precisely this strange magnitude-redshift diagram that has stimulated us to think about cosmological distance determinations for many years [9].

To evaluate the quasar data set, we first create 75 z-intervals with 1,773 quasars each. For these intervals we calculate the mean values $\langle z_i \rangle$ and the associated mean values $\langle m_i \rangle$ of the quasars. For all intervals we also calculate the standard deviations $\sigma_{m,\,i}$ and also the standard deviations $\sigma_{z,\,i}$. The latter, however, do not play a role in the analysis of the data set. The appendix contains the associated table, which also contains all $\sigma_{m,\,i}$.

Fig. 9 shows the magnitude-redshift diagram after averaging with all of the standard deviations $\sigma_{m,\,i}$ and $\sigma_{z,\,i}$ calculated by us.

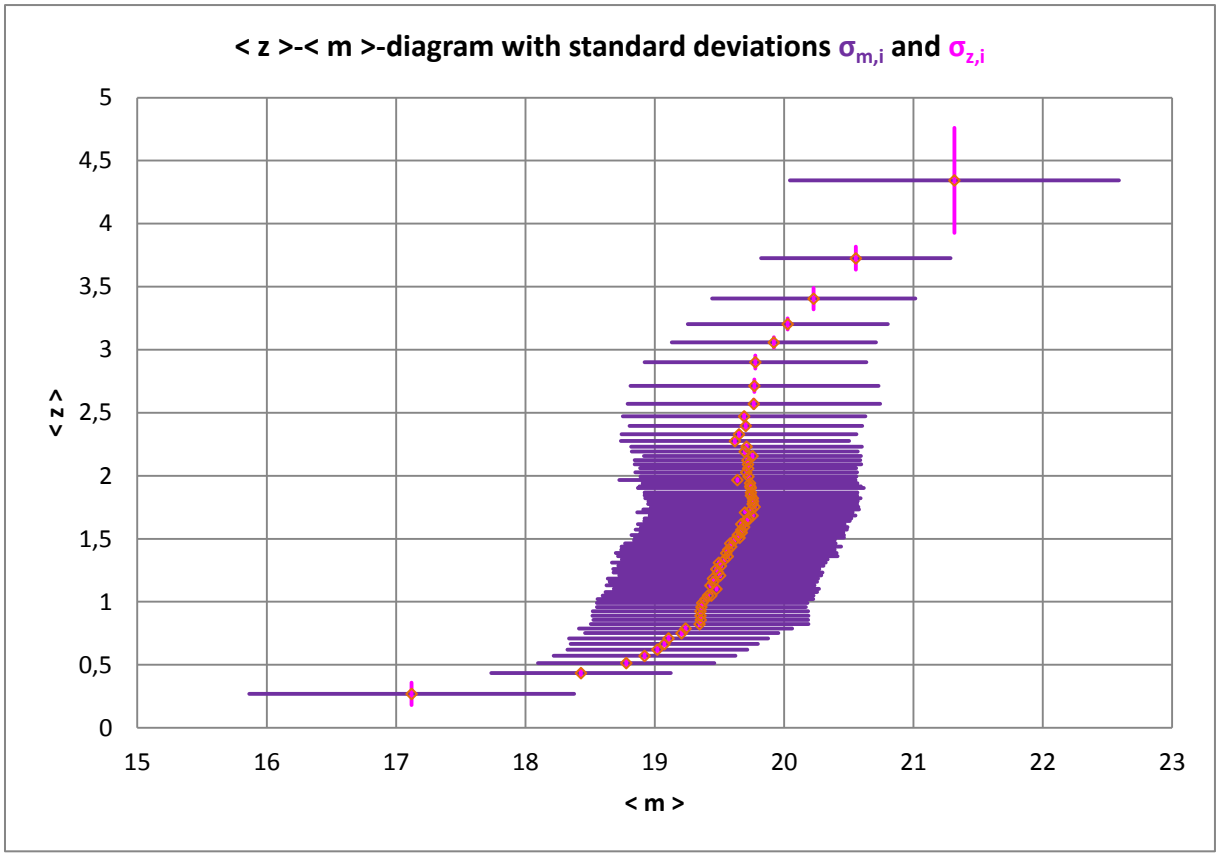

Figure 9. Magnitude-redshift diagram of the mean values $<z_i>$ and $<m_i>$ with inserted standard deviations $\sigma_{m,\,i}$ and $\sigma_{z,\,i}$.

The curvature of the curve expected on the basis of Fig. 8 can be clearly seen. This curvature should be explained by means of theory. More precisely: The theory has to explain the curvature!

We use the χ^2-function

$$\chi^2(p_k) = \sum_{i=1}^{N} \frac{\left[m_{th,i}(p_k) - m_{obs,i}\right]^2}{\sigma_{m,i}^{\;2}} \tag{53}$$

for the evaluation.

p_k with k = 1, 2 stands for the two parameters we are looking for, β_0 and m_{0a}.

If we use our magnitude-redshift relation (38), the result is concrete

$$\chi^2(\beta_0, m_{0a}) = \sum_{i=1}^{N} \frac{\left[5\log_{10}\left[\frac{1}{\beta_0}\left(1 - \frac{1}{\sqrt{1+z_i}} \right) + z_i \right] - 5\log_{10}(1+z_i) + m_{0a} - m_{obs,i} \right]^2}{\sigma_{m,i}^{\ 2}} \quad . \tag{53a}$$

Using the quasar data and using the usual mathematical procedure, we can find the parameters β_0 = 0.7311668 and m_{0a} = 20.1346.

Fig. 10 shows the result of the mean value formation and the adaptation of the theory to the curvature of the mean value curve.

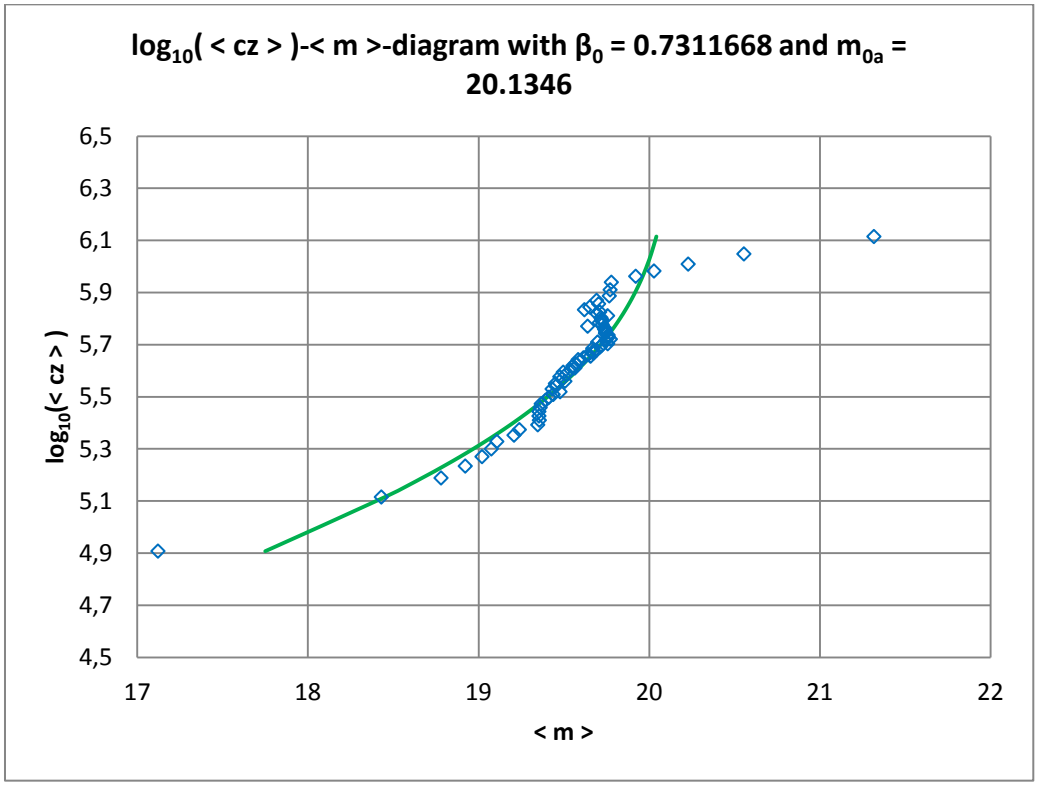

Figure 10. Magnitude-redshift diagram for 132,975 quasars according to M.-P. Véron-Cetty et al. [1].

To interpret the measured magnitude-redshift relation:

From our point of view, the quasars came in to being historically slowly as relatively weakly luminous objects at a point in time that corresponds to about $z \approx 4.3$. The quasars later behaved as the theory expects in flat space and moved with time - i.e. for decreasing redshifts z - on average along the theoretical curve (in the diagram from top right diagonally to bottom left). The quasars have gradually died out in the recent past and have become relatively bright in the process.

The dependence of the calculated standard deviations $\sigma_{m,\,i}$ on the redshift mean values $\langle z_i \rangle$ is shown in Fig. 11.

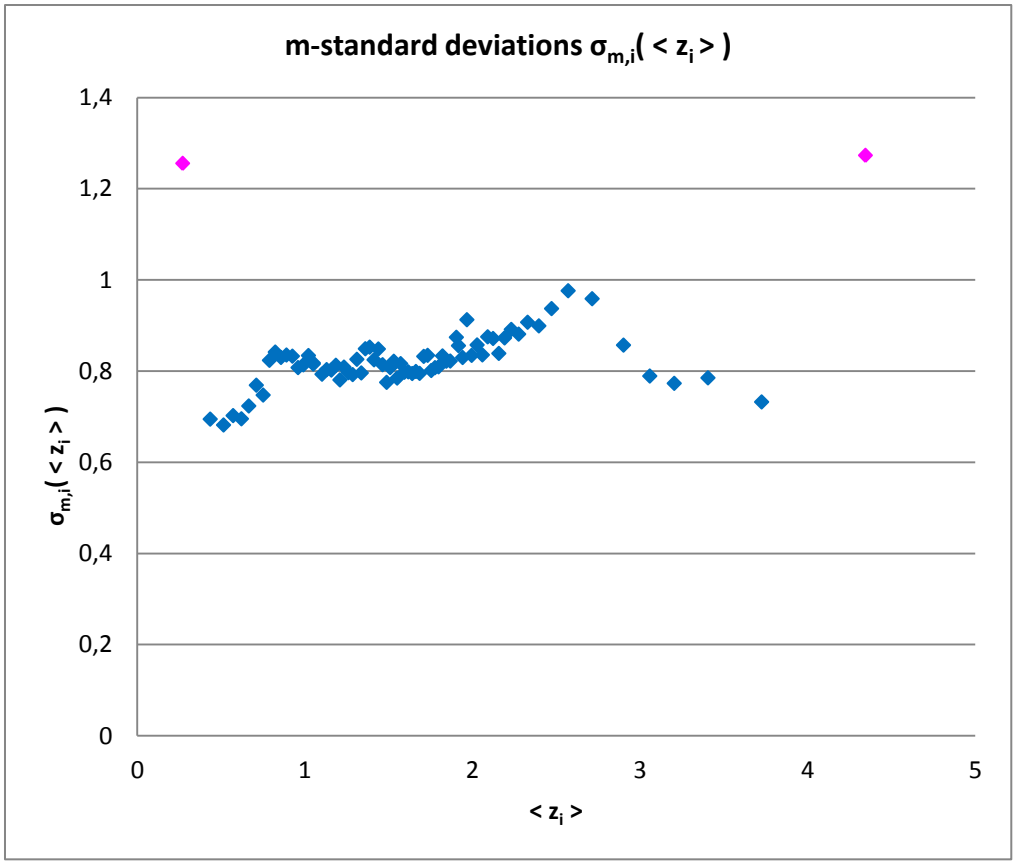

Figure 11. Standard deviations $\sigma_{m,\,i}$ as a function of $<z_i>$.

If we consider the first and last point in the diagram as outliers and therefore simply do not take them into account when evaluating the magnitude-redshift diagram of the quasars, we find the parameters $\beta_0 = 0.5486497$ and $m_{0a} = 19.9555$ for the values.

Because of the differences to the values mentioned above, we might come up with the idea of taking the mean values of each of these. But we will not do that in the following.

4.2 Number-redshift relation

We use the following χ^2-function to evaluate the number-redshift relation

$$\chi^2(p_k) = \frac{1}{N-1}\sum_{i=1}^{N}\left[N_{th,i}(p_k) - N_{obs,i}\right]^2 \quad . \tag{54}$$

p_k with k = 1, 2 stands for the two parameters we are looking for, β_0 and N_{0a}.

If we insert our number-redshift relation (46), the result is concrete

$$\chi^2(\beta_0, N_{0a}) = \frac{1}{N-1}\sum_{i=1}^{N}\left\{3\log_{10}\left[\frac{1}{\beta_0}\left(1-\frac{1}{\sqrt{1+z_i}}\right)+z_i\right]-3\log_{10}(1+z_i)+\log_{10} N_{0a}-N_{obs,i}\right\}^2 \quad . \qquad (54a)$$

Using simple mathematics, we find N_{0a} = 146,816 for the theoretically expected total number of quasars, if we use the value β_0 = 0.7311668 found via the magnitude-redshift relation.
The expected number is slightly larger than the actual number of quasars measured. This indicates a certain incompleteness of the measurements.

Fig. 12 shows the graphic result.

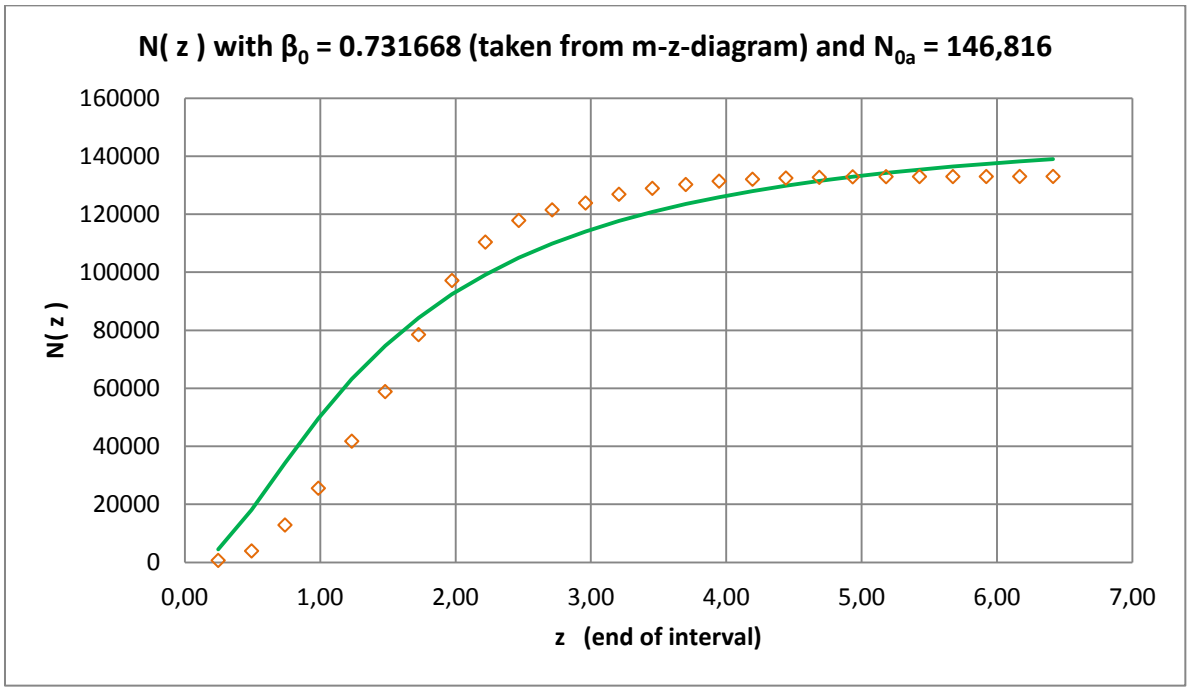

Figure 12. Number-redshift diagram for the 132,975 quasars according to M.-P. Véron-Cetty et al. [1].

Another possibility is to determine both parameters directly via the number-redshift relation, i.e. not to use the value of β_0 from the magnitude-redshift diagram of the quasars. This leads to the parameter values N_{0a} = 159,140 and β_0 = 0.8653211. Both values are slightly larger than those noted above.

Overall, we could build a mean value using three different values of β_0. However, we will not make use of this possibility in the following.

4.3 Angular size-redshift relation

We use the measurement data from K. Nilsson et al. [2] to find an average linear size of the cosmic objects measured there.

The starting point is the χ^2-function

$$\chi_\varphi{}^2(p_k) = \frac{1}{N-1}\sum_{i=1}^{N}\left[\varphi_{th,i}(p_k) - \varphi_{obs,i}\right]^2 \quad . \tag{55}$$

Here, p_k with k = 1, 2 stands for the two parameters we are looking for, β_0 and δ / R_{0a}.

If we use our angular size-redshift relation (40), the result is concrete

$$\chi_\varphi{}^2\left(\frac{\delta}{R_{0a}}, \beta_0\right) = \frac{1}{N-1}\sum_{i=1}^{N}\left\{\frac{\delta}{R_{0a}}\frac{(1+z_i)}{\left[\frac{1}{\beta_0}\left(1-\frac{1}{\sqrt{1+z_i}}\right)+z_i\right]} - \varphi_{obs,i}\right\}^2 \quad . \tag{55a}$$

The comparison of the theory with the measurement data using $\beta_0 = 0.7311668$ results in a value of $\delta / R_{0a} = 6.06 \times 10^{-5}$.

Fig. 13 shows the graphic result.

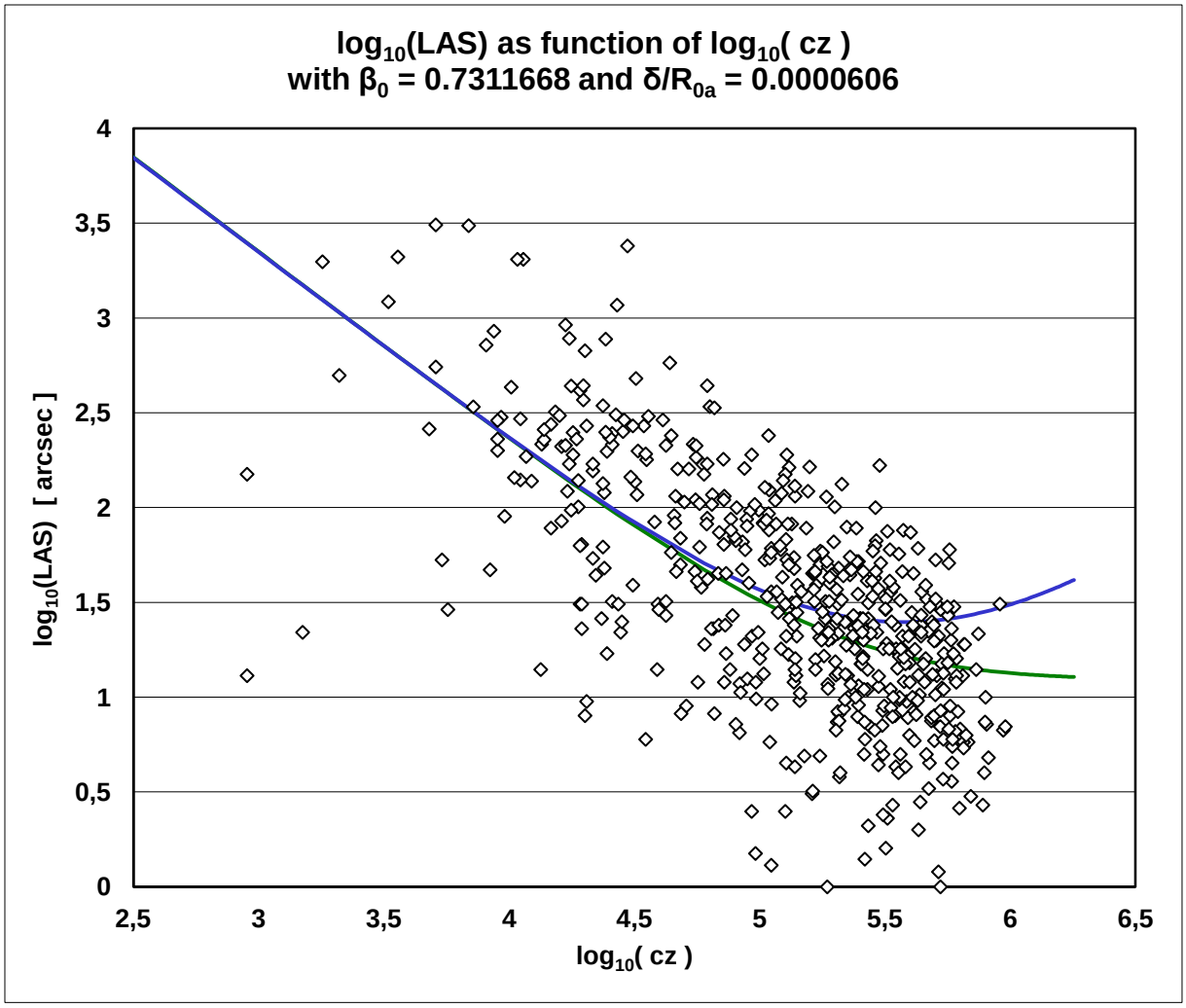

Figure 13. Angular size-redshift diagram according to K. Nilsson et al. [2].

For the purpose of comparison, the theoretical curve from the literature [see Eq. (63)] was drawn in. This curve cannot explain the position of the measured values in the diagram.

The determination of the linear size δ requires the knowledge of R_{0a}. Because the absolute magnitudes are known for some SNIa (which differ slightly from one another), we can determine R_{0a} using a magnitude-redshift diagram of these objects. We'll do that in the next chapter.

4.4 Fixing of R_{0a} with the help of SNIa

By W. L. Freedman et al. [3], data from a total of 27 SNIa were made available, with the help of which we can determine both the distance R_{0a} - a current distance - and, as a result, the today's Hubble parameter H_0.
The data we are interested in are the distance modules (μ_{TRGB} and μ_{Ceph}), the maximum apparent magnitudes (m_{CSP_B0} and m_{SC_B}) and the radial velocities V_{NED}, from which the redshifts z_{NED} can be calculated.

The methods taken into account in [3] for determining the maximum apparent magnitude and thus the associated absolute magnitude are different, which is why somewhat different values are given for one and the same SNIa. For our purposes, we calculate the mean values from these data and assign them to the relevant SNIa.

We calculate the absolute magnitudes M_i of the $SNIa_i$ using (μ_{TRGB} - m_{CSP_B0}) and (μ_{Ceph} - m_{SC_B}) and then always calculate an average value $<M_i>$ if both value pairs are specified for one and the same SNIa. From all the absolute magnitudes obtained in this way, we finally form the mean value of the absolute magnitude $<M> \approx -19.245$, which enables us to determine the distance R_{0a} with the aid of the parameter m_{0a}, which results from the magnitude-redshift diagram of the SNIa. The simple equation for this is

$$R_{0a} = 10^{\frac{m_{0a} - <M>}{5} + 1} \quad . \tag{56}$$

The graphic result is shown in Fig. 14.

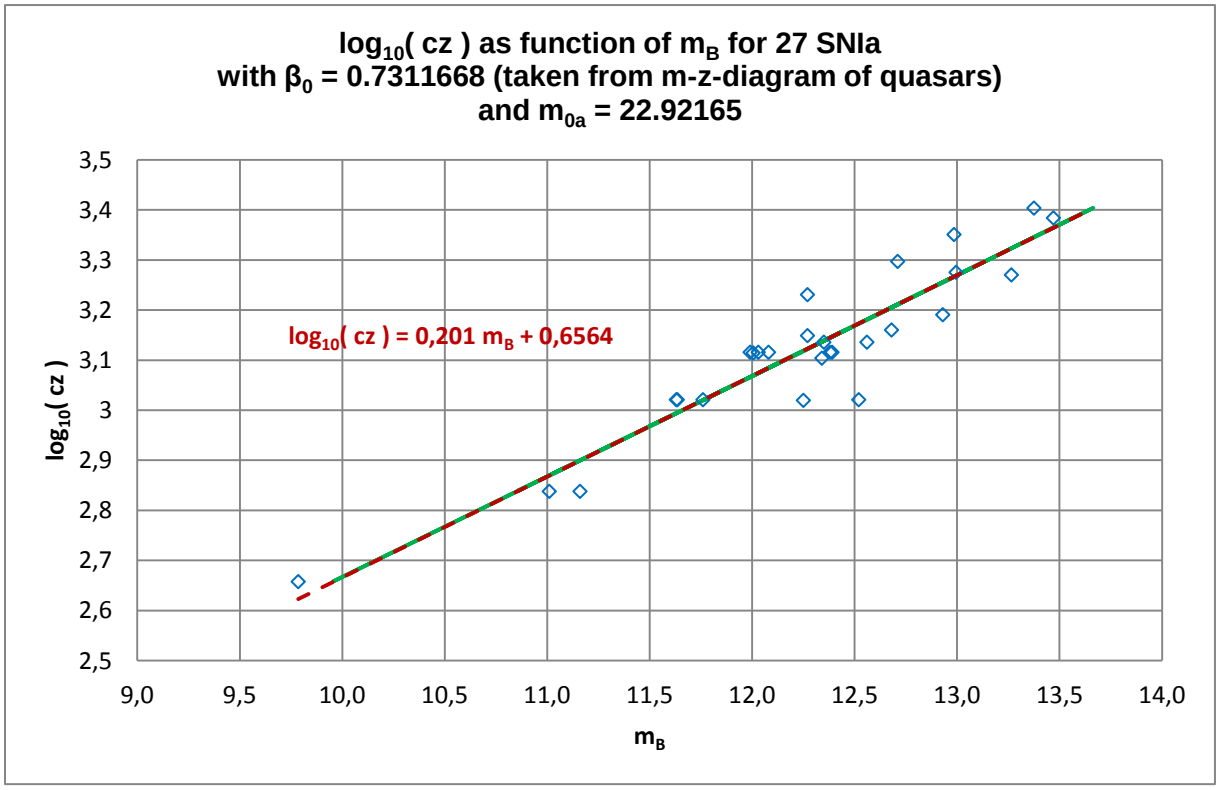

Figure 14. Magnitude-redshift diagram for 27 SNIa according to W. L. Freedman et al. [3].

The theoretical curve lies exactly on the linear trend line (dashed in red), the equation of which is given in the figure.

Using $m_{0a} \approx 22.922$ and the mean value of the absolute brightness $<M> = -19.245$, the distance $R_{0a} \approx 2{,}712.48$ Mpc we are ultimately looking for is the essential result of this data analysis.

With the help of the value of R_{0a} and using the equation (an approximation for small redshifts!)

$$H_{0a} \approx \frac{c}{\left(\frac{1}{2\beta_0}+1\right)R_{0a}} \tag{34}$$

the today's Hubble parameter $H_0 \approx 65.638$ km/(s Mpc) results. This value is slightly below the Planck value (2018) with $H_{0,\,Planck} \approx 67.66$ km/(s Mpc) [4].

In Table 8 in the appendix, all the values we used for the magnitude-redshift diagram of the 27 SNIa are compiled.

Starting from the equation

$$\frac{1}{\beta_0} = \frac{2c}{R_{0a}\sqrt{\frac{8\pi G \rho_0}{3}}} \tag{30}$$

Eq. (57) results for today's mass density:

$$\rho_0 = \frac{3}{2\pi}\frac{c^2}{G}\frac{{\beta_0}^2}{{R_{0a}}^2} \quad . \tag{57}$$

With the theoretical parameters, β_0 and R_{0a} determined by us, we find $\rho_0 \approx 4.843 \times 10^{-27}$ g/cm^3 for today's matter density in the universe.

Via

$$M_{Fs} = \frac{4\pi}{3}{R_{0a}}^3\rho_0 = \frac{4\pi}{3}{R_{0a}}^3\frac{3}{2\pi}\frac{c^2}{G}\frac{{\beta_0}^2}{{R_{0a}}^2} \qquad i.e. \qquad M_{Fs} = \frac{2c^2}{G}{\beta_0}^2 R_{0a} \tag{58}$$

the constant mass of the Friedmann sphere results in $M_{FS} \approx 1.206 \times 10^{56}$ g.

Because we generally do not consider the accuracy here, we simply specify the decimal places with up to 3 places, whereby the mathematical analysis of the data usually delivers more decimal digits.

Using Eq. (35) we find for the Schwarzschild radius $R_S \approx 5{,}800.43$ Mpc and the speed which is contained in Eq. (30) results in $V_0 \approx 219{,}198.29$ km/s.

With the known value $R_{0a} \approx 2{,}712.48$ Mpc we can calculate the mean linear size of the Nilsson objects [2] to be $\delta \approx 0.164$ Mpc, because we have found $\delta / R_{0a} = 6.06 \times 10^{-5}$ for them.

Using R_{0a} and β_0, of course, all linear dimensions of these objects can be calculated using their angular size and redshift.

4.5 Calculation of the further redshift distances for the SNIa and M87

Because we were able to determine R_{0a}, we can graphically display the further redshift distances in a form that is not normalized to R_{0a}. The result is shown in Fig. 15, using the values we found for β_0 and R_{0a}.

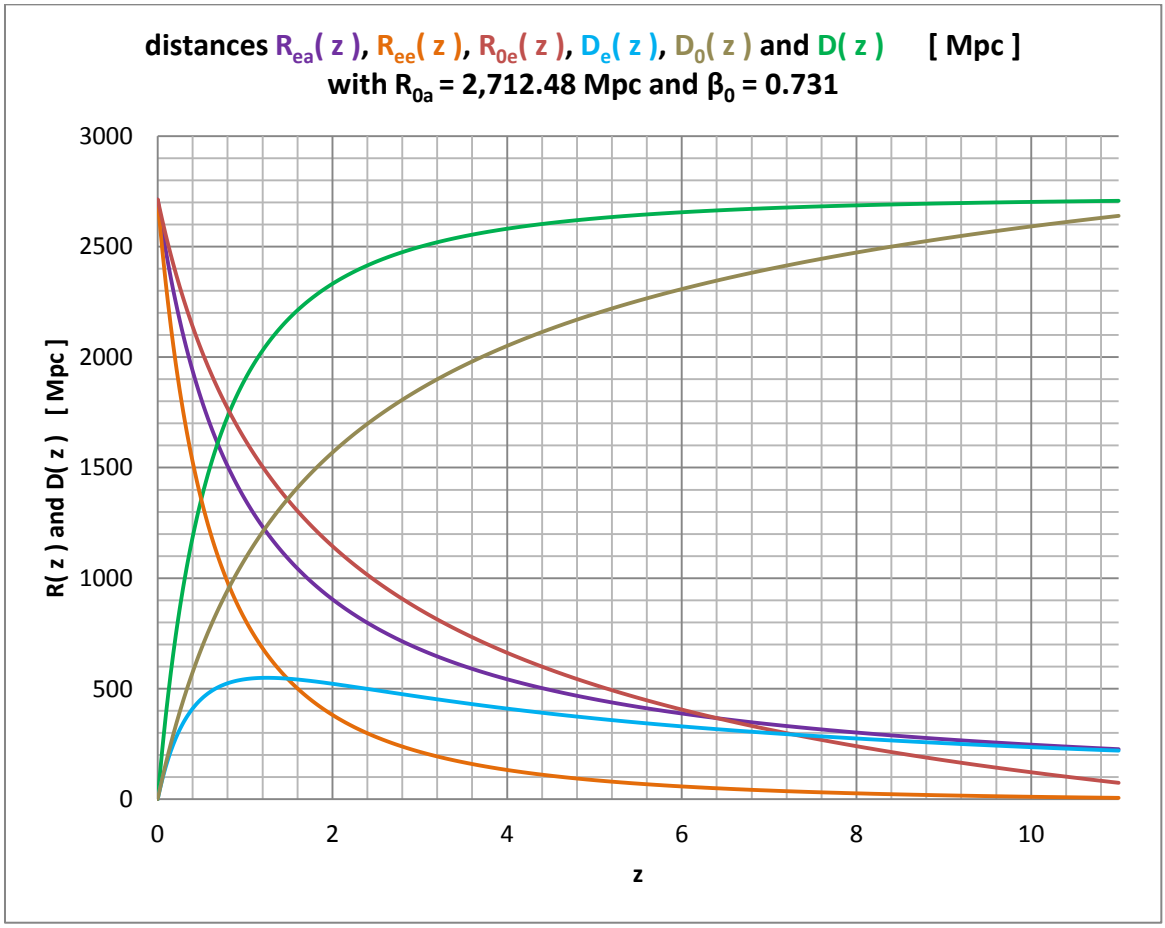

Figure 15. Redshift distance D (light path) and the further redshift distances D_i (i = 0, e) and R_{jk} (j = 0, e; k = e, a) as a function of the redshift up to z = 11.

To interpret Fig. 15:

a) For D -> R_{0a} the redshift z goes towards infinity. This means that no observer can observe objects for which is $D \geq R_{0a} \approx 2{,}712.48$ Mpc.

b) The light path distance $D = R_{0a} - R_{ee}$ is always greater than the distance differences D_0 (today) and D_e (then). In particular, the light path D is not equal to the today's distance D_0 between the two astrophysical objects.

c) The distances R_{jk} are physical distances from a coordinate origin and develop directly with the change in the scale parameter a(t) over time. For large redshifts, the scale parameter was correspondingly small and, as a result, the associated distances were also correspondingly small.

d) The distance D_e at the that time (t_e) is interesting: It shows a maximum for a specific redshift and only approaches zero for very large redshifts. This is also the reason for the further approximation of D_0 to D only for very large redshifts.

Table 1 summarizes all calculated redshift distances of the 27 SNIa [Mpc].

SNIa	R_{ea}	R_{ee}	R_{0e}	R_{0a}	D_e	D_0	D
1980N	2,700.72	2,692.70	2,704.43	2,712.48	8.02	8.05	19.78
1981B	2,703.02	2,696.56	2,706.00	2,712.48	6.46	6.48	15.92
1981D	2,700.72	2,692.70	2,704.43	2,712.48	8.02	8.05	19.78
1989B	2,706.26	2,702.02	2,708.23	2,712.48	4.25	4.26	10.47
1990N	2,703.02	2,696.56	2,706.00	2,712.48	6.46	6.48	15.92
1994D	2,703.02	2,696.56	2,706.00	2,712.48	6.46	6.48	15.92
1994ae	2,698.51	2,689.00	2,702.92	2,712.48	9.52	9.57	23.49
1995al	2,695.53	2,683.98	2,700.87	2,712.48	11.54	11.61	28.50
1998aq	2,700.16	2,691.76	2,704.05	2,712.48	8.40	8.44	20.72
1998bu	2,706.26	2,702.02	2,708.23	2,712.48	4.25	4.26	10.47
2001el	2,703.04	2,696.60	2,706.02	2,712.48	6.44	6.46	15.88
2002fk	2,695.72	2,684.31	2,701.00	2,712.48	11.41	11.48	28.17
2003du	2,690.74	2,675.97	2,697.59	2,712.48	14.78	14.90	36.51
2005cf	2,692.33	2,678.63	2,698.68	2,712.48	13.70	13.81	33.86
2006dd	**2,700.72**	**2,692.70**	**2,704.43**	**2,712.48**	**8.019**	**8.054**	**19.78**
2007af	2,694.66	2,682.53	2,700.27	2,712.48	12.13	12.21	29.95
2007on	2,700.72	2,692.70	2,704.43	2,712.48	8.02	8.05	19.78
2007sr	2,697.17	2,686.74	2,702.00	2,712.48	10.43	10.49	25.74
2009ig	2,689.75	2,674.30	2,696.90	2,712.48	15.45	15.58	38.18
2011by	2,700.16	2,691.76	2,704.05	2,712.48	8.40	8.44	20.72
2011fe	2,708.37	2,705.56	2,709.67	2,712.48	2.81	2.81	6.92
2011iv	2,700.72	2,692.70	2,704.43	2,712.48	8.02	8.05	19.78
2012cg	2,703.02	2,696.56	2,706.00	2,712.48	6.46	6.48	15.92
2012fr	2,700.75	2,692.76	2,704.45	2,712.48	7.99	8.03	19.72
2012ht	2,699.45	2,690.58	2,703.56	2,712.48	8.88	8.92	21.91
2013dy	2,699.79	2,691.13	2,703.79	2,712.48	8.65	8.69	21.35
2015F	2,701.03	2,693.23	2,704.64	2,712.48	7.81	7.84	19.26

Table 1. Redshift distance D and the further redshift distances D_i and R_{jk} of all 27 SNIa.

To interpret the distances from Table 1:

For a more detailed explanation, we take the SNIa **2006dd**, for example, and use it to interpret the meaning of the distances in the table.

The "light-travel time" always means the time interval between the emission of light (time $t_{e,\ 2006dd}$) by the SNIa 2006dd and today (t_0), i.e. $\Delta t = t_0 - t_{e,\ 2006dd}$. This light-travel time is generally different for all observable cosmic objects, here especially for the individual SNIa we have considered.

a) Today's (t_0) distance between the selected SNIa and us as observers is $D_0 \approx 8.054$ Mpc.

b) The then (t_e) distance between this SNIa and us as observers was $D_e \approx 8.019$ Mpc.

According to this, the distance between the two cosmic objects has increased by about 0.035 Mpc during the light-travel time $\Delta t = t_0 - t_{e,\ 2006dd}$.

c) The SNIa has been shifted expansively away from the origin of the coordinates by $\Delta R_e = R_{0e} - R_{ee} \approx 11.73$ Mpc during the light-travel time due to the time-dependent scale parameter a(t).

d) The galaxy with us as observers has been expansively shifted away from the origin of the coordinates by $\Delta R_a = R_{0a} - R_{ea} \approx 17.765$ Mpc during the light-travel time due to a(t).

The difference between the two displacement distances is of course the increase in the distance between the two cosmic objects noted above.

e) The light path covered by the photons within the time $\Delta t = t_0 - t_{e,\ 2006dd}$ (redshift distance) is $D \approx 19.78$ Mpc. It is unequal to the other mentioned distances D_i and greater than these.

4.6 Evaluation of the data from the black hole in M87

For the sake of simplicity, we summarize the data taken from the literature on the galaxy M87 with the black hole (BH) in it in the first line of Table 2 {see [5] and [6]}.

The second line lists the data specified here, which usually differ from those in the literature.

	D [Mpc]	**M_B [mag]**	**z**	**m_B [mag]**	**Θ_{BH} [µas]**	**$\delta/2 = R_S$ [pc]**	**M_{BH} [g]**
literature	16.9 / 16.8	-23.5	0.004283	9.6	42		1.2928E+43
we	19.45	-21.84				0.227	2.3584E+45

Table 2. Summary of data from galaxy M87 with the black hole in it.

The theory was adapted to the measured angle size Θ_{BH} from the literature. Overall, a larger redshift distance D, a smaller absolute magnitude M_B and a significantly larger mass M_{BH} of the black hole follow.

Table 3 lists the values found by means of our theory for all redshift distances R_{jk}, D_i and for D.

[Mpc]	R_{ea}	R_{ee}	R_{0e}	R_{0a}	D_e	D_0	D
we	2,700.92	2,693.03	2,704.56	2,712.48	7.89	7.92	19.45
literature	---	---	---	---	---	---	16.8

Table 3. Redshift distances D_i, D and R_{jk} from the black hole in M87.

From these values, the expansion-related shifts in distance of the galaxy M87 and of the galaxy with us as observers can be calculated, which took place during the time of light travel.

The theory from the literature does not know the first 6 listed distances. It can therefore not be calculated using this theory and also not determine in terms of value.

The distance D differs because of the physical meaning: In our theory, D is the real physical light path, which is not the case in the literature.

We briefly interpret the meaning of the distances in Table 3, whereby the light-travel time is again defined as above:

a) Today's (t_0) distance between the black hole (BH) or the galaxy M87 and us as observers is $D_0 \approx 7.92$ Mpc.

b) The then (t_e) distance between the BH (or M87) and us as observers was $D_e \approx 7.89$ Mpc.

Accordingly, the distance between the two cosmic objects has increased by about 0.03 Mpc during the light-travel time $\Delta t = t_0 - t_{e,\ BH,\ M87}$.

c) The BH (or M87) has been shifted expansively away from the origin of the coordinates by $\Delta R_e = R_{0e} - R_{ee} \approx$ 11.53 Mpc during the light-travel time due to the time-dependent scale parameter a(t).

d) The galaxy with us as observer was expansively shifted away from the origin of the coordinates by $\Delta R_a = R_{0a} - R_{ea} \approx 11.57$ Mpc during the light-travel time due to a(t).

e) The light path (redshift distance) covered by the photons during the time $\Delta t = t_0 - t_{e,\ BH,\ M87}$ is $D \approx 19.45$ Mpc. It is unequal to the other mentioned distances D_i and greater than these.

Fig. 16 shows the various calculated distances in a clear form.

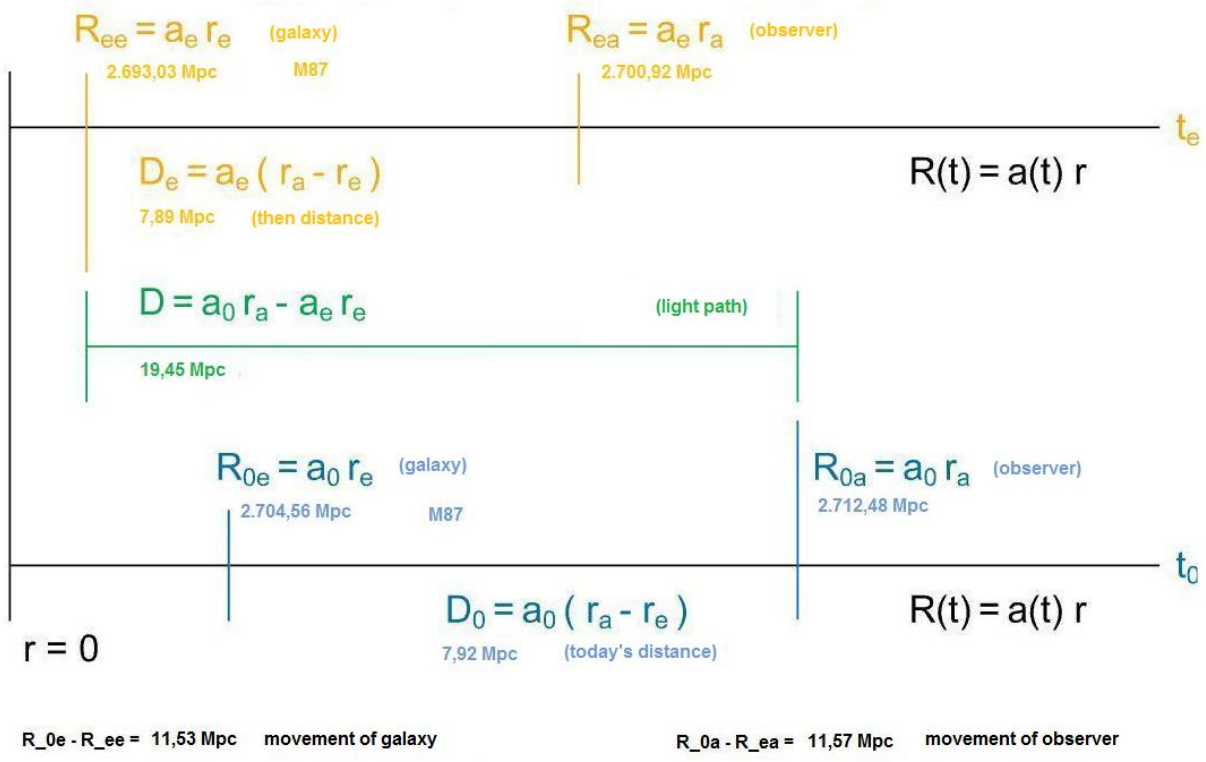

Figure 16. Visualization of the distances D_i, D and R_{jk} with regard to M87 and observer.

Note: The distances are not drawn to scale here.

4.7 Maximum values known today: Galaxy UDFj-39546284 and Quasar J0313

The galaxy UDFj-39546284 [8] currently holds the record among the galaxies with a redshift of z = 10.3, while the quasar J0313 [7] with z = 7.642 holds the analog record among the quasars.

Table 4 shows the corresponding distances R_{jk}, D_i and D together.

object name	z	D	D_0	D_e	R_{ee}	R_{0e}	R_{ea}	R_{0a}	object
J0313	7.642	2,681.858	1,789.782	207.103	30.622	264.636	313.872	2,712.480	quasar
UDFj-39546284	10.300	2,703.075	1,905.566	168.634	9.405	106.281	240.042	2,712.480	galaxy

Table 4. All calculated redshift distances R_{jk}, D_i and D for the two cosmic objects with the maximum redshifts.

Table 5 summarizes the spatial shifts of the objects with respect to the coordinate origin due to the expansion during the associated light travel times.

object name	$R_{0e} - R_{ee}$	$R_{0a} - R_{ea}$	object
J0313	234.014	2,398.608	quasar
UDFj-39546284	96.876	2,472.438	galaxy

Table 5. Expansion-related shifts in the distance of the quasar and the galaxy.

We have already explained above how the tables are to be interpreted.

Fig. 17 shows the distances D_i and D of the 3 special astrophysical objects analyzed here in one diagram, whereby we have entered all numerical values for the distances in Mpc.

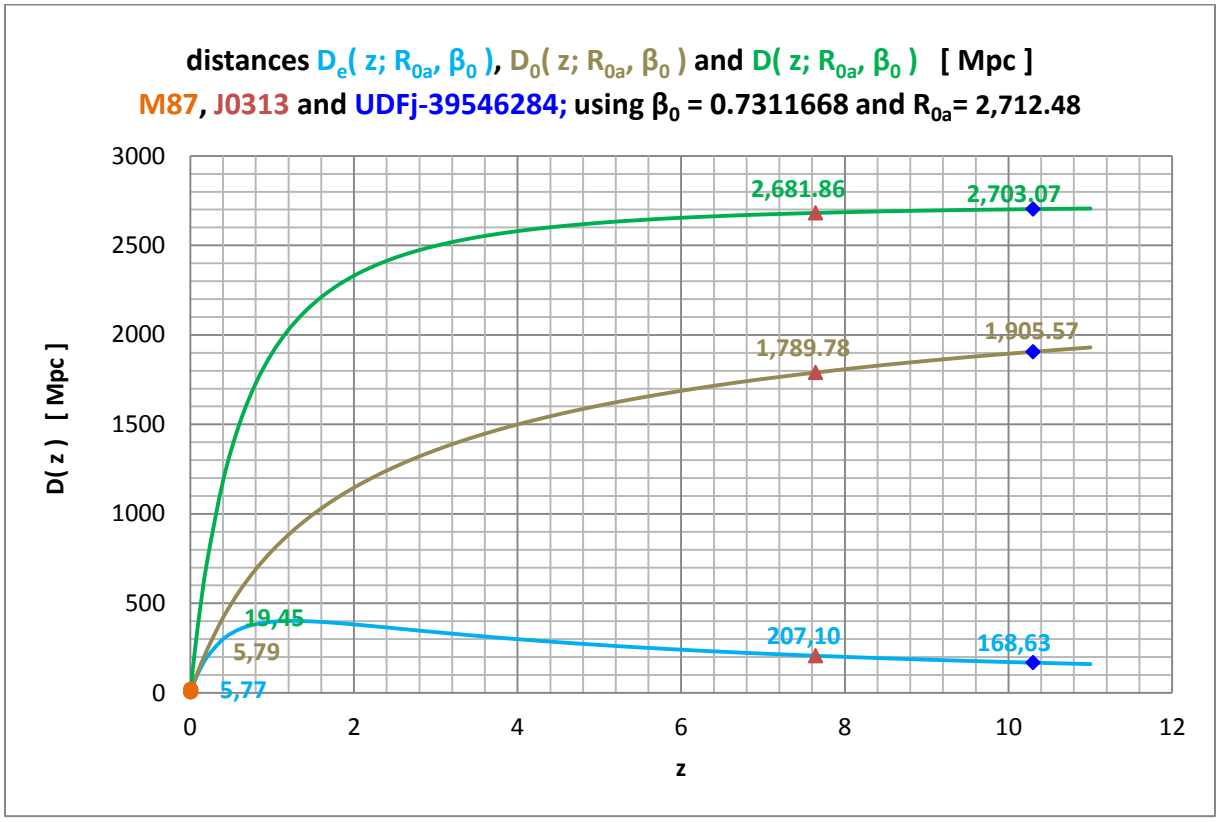

Figure 17. All distances D_i and D for M87, J0313 and UDFj-39546284.

The middle curve shows the current distances D_0 of the objects from us as observers. These distances are clearly smaller than the associated light paths D.

5 Additions

5.1 About the mass of Friedmann sphere

The cause of the expansion of the universe visible to us as observers is its constant mass M or the time-varying density $\rho_M(t)$, respectively. It ensures that the scale parameter changes over time. To check this statement, simply set the matter density in the Friedmann equation to zero.

Every cosmologist therefore has to ask himself where exactly this mass is located in the universe. He can gain an answer for this by borrowing the appropriate ideas from classical non-relativistic Newtonian cosmology. There he has to imagine a mass sphere whose radius changes over time (e.g. grows). This means that the mass in question is completely within this sphere, and it is evenly distributed and remains there according to the cosmological principle. In relativistic cosmology, the time depend product of scale parameter and coordinate distance R(t) = a(t) r takes over the role of the physical radius of the mass sphere, and it holds that the entire mass to be considered is inside this sphere (Friedmann sphere named here).

Incidentally, the Friedmann equation of the flat universe looks strangely exactly as the equation of the non-relativistic Newtonian cosmology. There is no relativity seen in the equation e.g. in the sense of limiting the rate of change da/dt of the scale parameter to the speed of light.

The Fig. 18 shows the projection of a Friedmann sphere in to the plane at time t_0 (today) in which examples of possible places for an observer and galaxy observed are drawn.

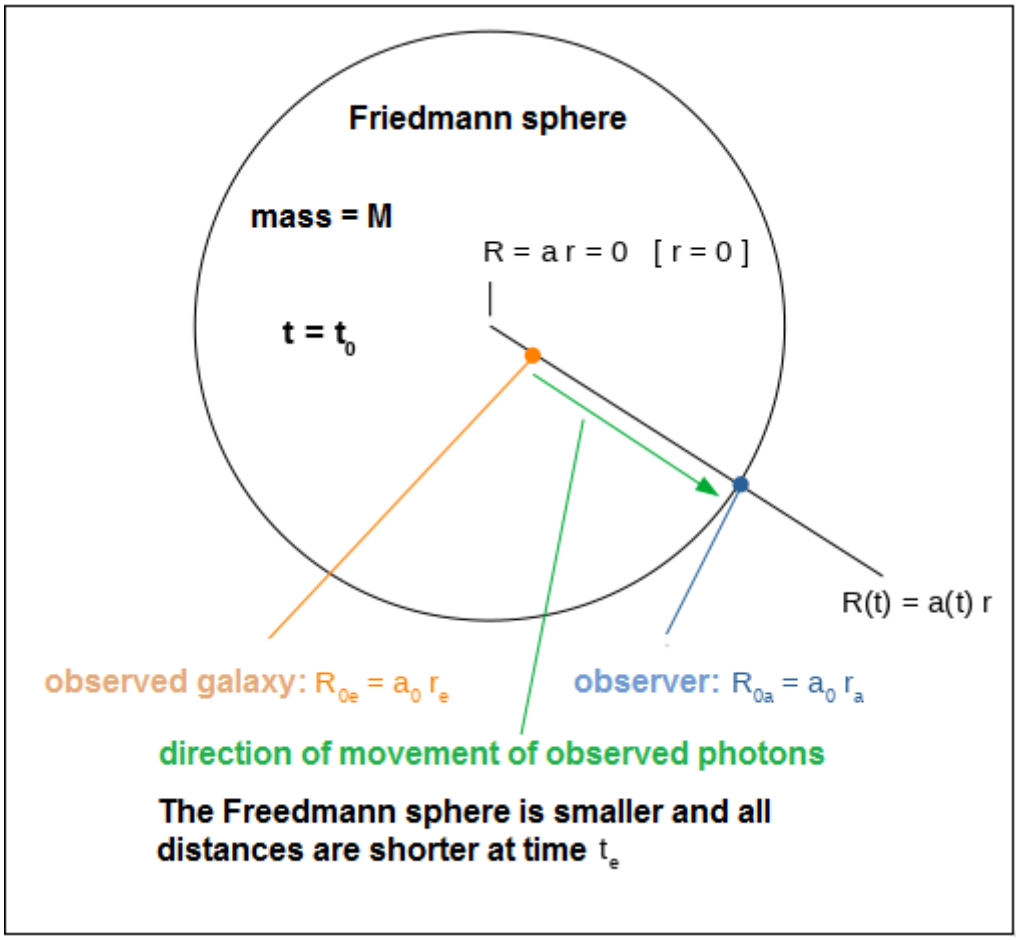

Figure 18. Friedmann sphere with examples of physical locations of an observer and a galaxy.

Because of the law of conservation of mass

$$M = \frac{4\pi}{3}\rho_0 {a_0}^3 {r_a}^3 = \frac{4\pi}{3}\rho_0 {R_{0a}}^3 \tag{36a}$$

which is used here we see that R_{0a} is today's radius of the Friedmann sphere with today's mass density ρ_0.

An observable galaxy can minimally have the co-moving coordinate with $r_e = 0$. If a galaxy is placed there, we observe an infinitely large redshift for such a galaxy according to our redshift distance. For all other locations $r_e \neq 0$ of an observed galaxy, a smaller redshift is always measured.

Because an infinitely large redshift is always observed for the light path $D = R_{0a}$, it can be assumed that in the physical radius $R_{0a} = a_0 r_a$ of a Friedmann sphere, the co-moving coordinate r_a has the maximum possible value $r = 1$ according to the complete FLRWM. R_{0a} therefore describes the maximum size of the Friedmann sphere, which of course is time-dependent. This maximum value of the co-moving and dimensionless radial coordinate r follows from the FLRWM with positive curvature $\varepsilon = 1$ and, from our point of view, can theoretically not simply be neglected despite the flat space-time assumed for today's universe.

Of course, each observer can also e.g. look in exactly the opposite direction to the direction shown (green arrow). In this case, he looks again into a Friedmann sphere, which belongs to this direction. For $D = R_{0a}$ there is also an infinite redshift in this direction. The observer can of course also look in any other directions. The observer always looks into Friedmann spheres, which of course partially overlap.

Overall, there is a part of the universe with a spherical radius R_{0a}, that is visible to any observer. A universe thought to be spherical corresponds to at least one sphere with the radius $2 \cdot R_{0a}$, since beyond R_{0a} there is always also mass. Every observer sits on the surface of Friedmann spheres. Nevertheless, he can believe that his place is also in a center of such a Friedmann sphere.

If we would put the position of an observer a little outside the Friedmann sphere shown in Fig. 18, he would find the same situation as described above, if the universe would be actually much larger than a sphere with the radius $2 \cdot R_{0a}$ or even infinitely large.

5.2 About the derivation of the redshift distance in the literature

In the literature, the observer is usually placed in the coordinate origin $r_a = 0$ (see Fig. 19). Because of $r_e \geq r_a = 0$, this results in the light path simply as $D_{literature} = a_0 r_e$. This depends only on the co-moving coordinate location r_e of the observed galaxy and on the today's value of the scale parameter a_0. An earlier scale parameter such as a_e does not play a role in this approach, which we consider as a strong limitation of the generality.

In this case, the photons run inside a mass sphere from the outside to the inside, i.e. always towards the origin $r_a = 0$ (incoming photons). Any other way of defining $D_{literature}$ would be physically nonsense.

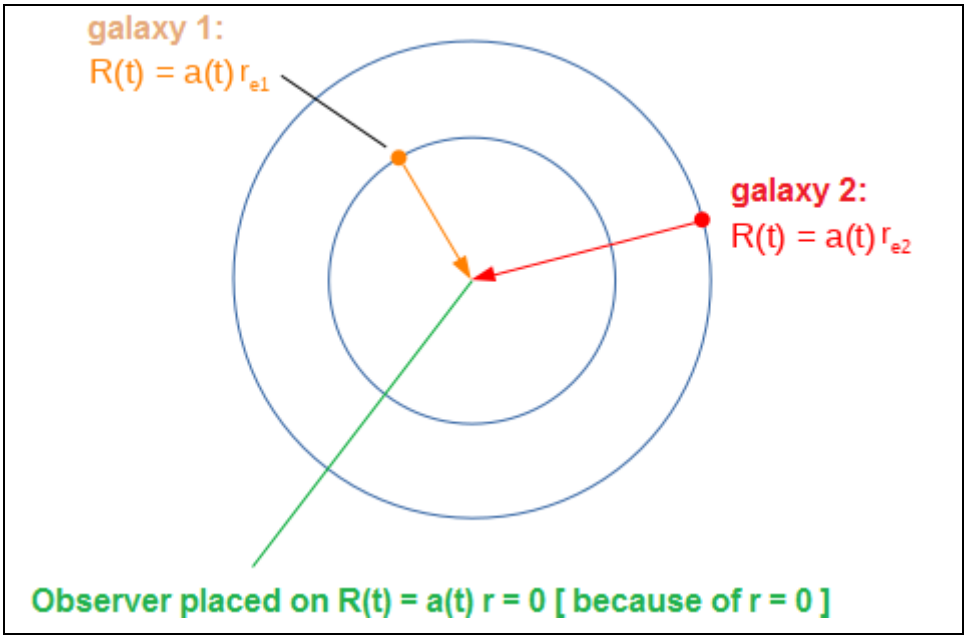

Figure 19. Observer generally placed on the center of the co-moving coordinate system ($r_a = 0$).

The calculation analogous to our derivation of the redshift distance (see chapter 2.2) results first in

$$D_{literature}(z; a_0, R_S) = D_0 \frac{\left(1+z-\sqrt{1+z}\right)}{(1+z)} \qquad with \qquad D_0 = 2\,a_0 \sqrt{\frac{a_0}{R_S}} \quad . \tag{59}$$

We have denoted the index of the maximum distance for which $z = \infty$ is reached with 0, because the calculation based on $D_{literature, i} = a_0\, r_{e,i}$ generally gives the today's distance between any galaxy i and any observer.

In the literature, the magnitude distance is indicated with

$$D_m = (1+z) D_{literature} \quad , \tag{60}$$

whereby with the help of factor (1 + z) an overall thinning of the number of photons due to the enlargement of the spherical area on which the radiation hits after its way through the universe and the energy loss due to the redshift is taken into consideration.

So it results first in

$$D_m(z;a_0,R_S)=2a_0\sqrt{\frac{a_0}{R_S}}\left(1+z-\sqrt{1+z}\right) \tag{61}$$

or

$$D_m(z;a_0,R_S)=2a_0\sqrt{\frac{a_0}{R_S}}(1+z)\left(1-\frac{1}{\sqrt{1+z}}\right) \quad . \tag{61a}$$

Here, too, the prefactor is a distance parameter for which can be introduced an apparent magnitude.

If, in a case which is also possible, the observed galaxy (each one because there are many; see Fig. 20) each placed to its own coordinate origin (outgoing photons), the result of calculation - for obvious reasons of symmetry - is of course the same redshift distance as above. This can easily be checked by means of an elementary calculation.

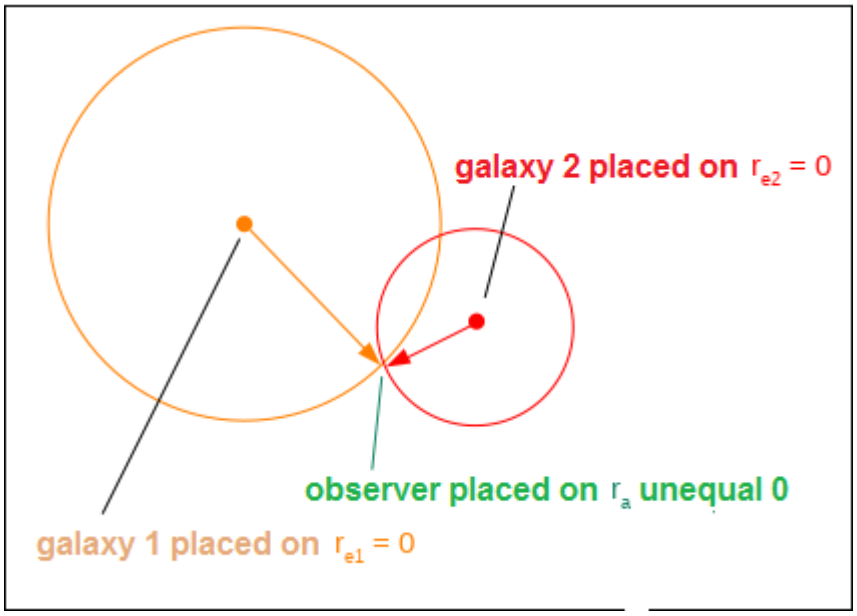

Figure 20. Observed galaxies (i = 1, 2) each in their own coordinate origin ($r_{e,i} = 0$).

Therefore, this results for the magnitude-redshift relation in

$$m_{literature}(z;m_{D_0})=5\log_{10}\left(1-\frac{1}{\sqrt{1+z}}\right)+5\log_{10}(1+z)+m_{D_0} \quad . \tag{62}$$

For the angular size-redshift relation we find

$$\log_{10}\varphi_{literature}(z;\delta/D_0)=\log_{10}\frac{\delta}{D_0}-\log_{10}(1+z)-\log_{10}\left(1-\frac{1}{\sqrt{1+z}}\right)\quad . \tag{63}$$

For the number-redshift relation we get accordingly

$$\log_{10} N_{literature}(z;N_0)=3\log_{10}\left(1-\frac{1}{\sqrt{1+z}}\right)+3\log_{10}(1+z)+\log_{10} N_0\quad . \tag{64}$$

All three equations also result from the well-known Mattig equation (1958), if the delay parameter $q_0 = 1/2$ is set there, whereby this equation describes a flat universe {see e.g. A. R. Sandage et al. [10]}.

We have used Eq. (63) in the measured value diagram Fig. 13 for comparison with the theory presented here.

5.3 Consideration of the radiation density in the early days of cosmological expansion

When deriving the redshift distance in chapter 2.2, we neglected the relativistic radiation density ρ_R that was originally dominant in the early days of the universe. The reason for this is that today, actually for several billion years, this density no longer plays a role in the further development of the universe over time due to its small value compared to the non-relativistic mass density ρ_M.

If this radiation density is taken into account from the start when deriving the redshift distance according to the scheme in chapter 2.2 the result is a more complex redshift distance because it then also dependent on a further parameter:

$$D_{RM}(z;R_{0a},\beta_{0,RM},\Omega_{0,RM})=\frac{R_{0a}}{(1+z)}\left\{\frac{1}{\beta_{0,RM}}\left[1-\frac{\sqrt{\Omega_{0,RM}+\frac{1}{(1+z)}}}{\sqrt{1+\Omega_{0,RM}}}\right]+z\right\}\quad .$$

$$with\qquad R_{0a}=a_0 r_a\qquad and\qquad \frac{1}{\beta_{0,RM}}=2\sqrt{\frac{R_{0a}}{R_S}}\sqrt{1+\Omega_{0,RM}}\qquad and\qquad \Omega_{0,RM}=\frac{\rho_{0,R}}{\rho_{0,M}} \tag{65}$$

$$index\ 0:today\qquad index\ R:radiation\qquad index\ M:non-relativistic\ matter$$

Here the current density quotient $\Omega_{0,RM}$ is included as a further parameter, which takes into account the very early radiation era. For today's radiation density, the designation $\rho_{0,R}$ was introduced again and today's non-relativistic mass density was named $\rho_{0,M}$. The parameter $\beta_{0,RM}$ corresponds to our parameter β_0 in Eq. (31).

With the numerical values for today's density quotient $\Omega_{0,RM}$ mentioned in chapter 1, it can be seen immediately that $\rho_{0,R}$ or $\Omega_{0,RM}$ can actually be neglected.

In addition, when comparing Eq. (65) with the measured values (e.g., magnitude-redshift diagram of the quasars), there is no longer any effect fitting the measurement curve for a density quotient smaller then $\Omega_{0,RM} \approx 0.01$.

If we set $\Omega_{0,RM} = 0$ in Eq. (65) - this corresponds to our neglect of today's radiation density $\rho_{0,R}$ - we get Eq. (31) again. Accordingly, this Eq. (31) is actually valid as today's redshift distance, containing the parameters R_{0a} and $\beta_{0,RM} = \beta_0$ only.

6. Final considerations

6.1 Hubble parameter

At this point we explicitly point out that our equation of today's Hubble parameter - which also only applies to very small redshifts - differs significantly from the definition (!) used in the literature:

$$H_{0a} \approx \frac{1}{\left(\frac{1}{2\beta_0}+1\right)}\frac{c}{R_{0a}} \qquad (we)$$

and

$$H_{0,lit} = \frac{\dot{a}_0}{a_0} = \frac{\dot{a}_0 r_a}{a_0 r_a} = \frac{\dot{R}_{0a}}{R_{0a}} \qquad r_a = const \qquad (literature) \quad . \tag{66}$$

For an arbitrary point in time t this is

$$H_a(t) \approx \frac{1}{\left(\frac{1}{2\beta(t)}+1\right)}\frac{c}{a(t)r_a} = \frac{1}{\left[\sqrt{\frac{a(t)r_a}{R_S}}+1\right]}\frac{c}{a(t)r_a} \qquad (we)$$

$$because\ of \qquad \frac{1}{\beta(t)} = 2\sqrt{\frac{a(t)r_a}{R_S}} \quad with \quad \frac{c}{r_a} = const \quad \frac{r_a}{R_S} = const \quad R_S = const \tag{66a}$$

and

$$H_{a,lit}(t) = \frac{\dot{a}(t)}{a(t)}\frac{r_a}{r_a} \qquad (literatur) \quad .$$

The index a generally indicates the proximity to the observer ($r = r_a$).

In our theory, the numerator contains the constant physical speed of light c in a vacuum, while the current, i.e. variable, spatial expansion speed (da/dt) can be found at this point in the literature.

In the more recent past - time t_x - our distance from the coordinate origin $R_{xa} < R_{0a}$ was slightly smaller than the current one and the Hubble parameter was therefore correspondingly larger (also via the parameter β_x).

In the case of the Hubble parameter in literature, the - actually non-physical - spatial expansion speed da/dt can have been arbitrarily large and, in addition, the scale parameter a(t) arbitrarily small.
Both types of Hubble parameters therefore show completely different behavior!

In addition, our Hubble parameter is actually made up of physical quantities, while the Hubble parameter in the literature is only defined using the non-physical scale parameter a(t), even if the latter can be assigned a suitable unit of measurement - e.g. Mpc. This means that a(t) per se is not a physical distance. This meaning only applies to the real physical distance R(t) = a(t) r and the differences that can be calculated from it.

The Hubble parameter is the proportionality factor between the Hubble speed V_H = cz and a distance, i.e. the actual Hubble law applies

$$V_H = cz = H_{0a} D \approx \frac{1}{\left(\frac{1}{2\beta_0} + 1\right)} \frac{c}{R_{0a}} D \qquad (we)$$

and (67)

$$V_{H,lit} = cz = H_{0,lit} D_{lit} = \frac{\dot{a}_0}{a_0} D_{lit} = \frac{\dot{R}_{0a}}{R_{0a}} D_{lit} \qquad (literature) \quad .$$

For the redshift z it simply follows

$$z = \frac{H_{0a}}{c} D \approx \frac{1}{\left(\frac{1}{2\beta_0} + 1\right)} \frac{D}{R_{0a}} \qquad (we)$$

and (68)

$$z = \frac{H_{0,lit}}{c} D_{lit} = \frac{\dot{a}_0}{c} \frac{D_{lit}}{a_0} = \frac{\dot{R}_{0a}}{c} \frac{D_{lit}}{R_{0a}} \qquad (literature) \quad .$$

In the literature, the redshift z is therefore dependent on the ratio of the current speed of the observer (his galaxy) related to the origin of the coordinates to the speed of light in the product with the ratio of an object distance D_{lit} and the current distance of the observer's galaxy from the origin of the coordinates.

Our redshift, on the other hand, is dependent on the ratio of the light path distance D and the current distance of the observer galaxy from the coordinate origin R_{0a} and is besides proportional to the factor that contains the parameter β_0.
Using the parameter β_0

$$\frac{1}{\beta_0} = 2\sqrt{\frac{R_{0a}}{R_S}} \qquad with \qquad R_S = \frac{2MG}{c^2} \tag{69}$$

we see in our case

$$z = \frac{H_{0a}}{c} D \approx \frac{1}{\left(\sqrt{\frac{R_{0a}}{R_S}} + 1\right)} \frac{D}{R_{0a}} \qquad (we) \quad , \tag{70}$$

i.e. an direct dependence on the Schwarzschild radius R_S, or more precisely on the ratio R_{0a} to R_S.

Overall, it is somewhat unclear in the literature what exactly corresponds to the distance D_{lit}. A example for this statement is, that the Eq. (66b) can also be written as

$$\dot{a}_0 = H_{0,lit} a_0 \qquad or \qquad \dot{R}_{0a} = H_{0,lit} R_{0a} \qquad (literature) \quad . \tag{66c}$$

Fig. 21 shows the difference between the non-approximated redshift distance D and the linear Hubble redshift distance that is approximated.

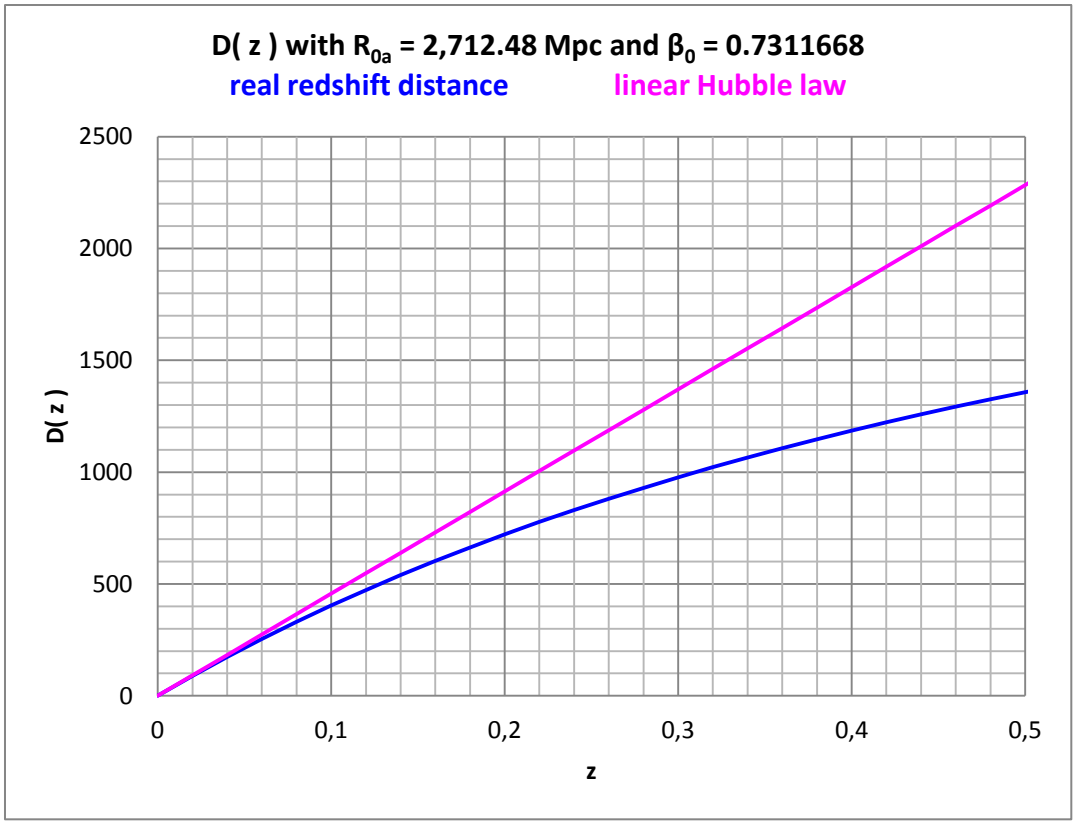

Figure 21. Non-approximated redshift distance D compared to the linear Hubble redshift distance.

It can be seen that the two curves already clearly separate from each other at $z \approx 0.03$, and that Hubble's law results in distances that are significantly too large for larger redshifts, so that it is no longer applicable from around this value.

Recall:
Of course, it should be noted that the Hubble parameter H_{0a} in our theory results from an approximation for small redshifts z.

6.2 Mean values

If we replace in the Eq. (38)

$$m(z; m_{0a}, \beta_0) = 5\log_{10}\left[\frac{1}{\beta_0}\left(1-\frac{1}{\sqrt{1+z}}\right)+z\right]-5\log_{10}(1+z)+m_{0a} \tag{38}$$

the parameter m_{0a} using Eq. (56a) containing the absolute magnitude M

$$m_{0a} = 5\log_{10}(R_{0a}) - 5 + M \qquad [R_{0a}] = pc \tag{56a}$$

we get

$$m(z; R_{0a}, \beta_0) = 5\log_{10}\left[\frac{1}{\beta_0}\left(1 - \frac{1}{\sqrt{1+z}}\right) + z\right] - 5\log_{10}(1+z) + 5\log_{10}(R_{0a}) - 5 + M \quad . \tag{71}$$

From this equation it follows immediately

$$R_{0a}(z; \mu, \beta_0) = \frac{(1+z)}{\left[\frac{1}{\beta_0}\left(1 - \frac{1}{\sqrt{1+z}}\right) + z\right]} 10^{\frac{\mu}{5}+1} \quad . \tag{72}$$

We have introduced the distance modulus $\mu = m - M$.

Note:
While the redshift z and the apparent magnitude m are actual measurable variables, the distance modulus μ has to be regarded as a parameter because the absolute magnitude M cannot be measured directly.

The parameter β_0 is known to us from the evaluation of the quasar catalog by Véron-Cetty [1]. In [3] the following parameters characterizing all 27 SNIa are given: absolute magnitude M_B, redshift z and maximum apparent magnitude m_B.
This allows us to calculate the associated $R_{0a,\,i}$ for all $SNIa_i$ (i numbers the individual SNIa). Table 6 shows the result:

z_i	$R_{0a,i}$ [Mpc]	z_i	$R_{0a,i}$ [Mpc]	z_i	$R_{0a,i}$ [Mpc]
0.00435635	2,685.59	0.00229826	2,989.52	0.00845251	2,160.13
0.00350242	2,620.06	0.00349242	3,130.03	0.00456316	2,811.99
0.00435635	2,685.59	0.00621763	3,059.04	0.00151772	2,602.36
0.00229826	2,868.15	0.00807892	2,850.38	0.00435635	2,636.57
0.00350242	3,608.37	0.00748518	2,242.44	0.00350242	2,749.87
0.00350242	2,699.68	0.00435635	2,685.59	0.00434300	2,543.10
0.00517691	3,137.28	0.00661458	2,079.37	0.00482667	2,956.51
0.00629102	2,821.83	0.00435635	2,636.57	0.00470325	2,488.62
0.00456316	3,069.12	0.00567726	2,088.18	0.00423960	2,902.49
< R_{0a} > =	**2,733.65**				

Table 6. Various distances $R_{0a,\,i}$ of the 27 $SNIa_i$ calculated using the distance modules μ_i.

It may seem strange that we get a different value for $R_{0a,\,i}$ for each $SNIa_i$, which is actually the current physical distance of the observer from the coordinate origin (r = 0). In particular, the $R_{0a,\,i}$ for almost equal redshifts z_i should match!
But if we form the mean value of the 27 calculated values $R_{0a,\,i}$, we find $\langle R_{0a} \rangle \approx 2{,}733.65$ Mpc. This value is very close to the value $R_{0a} \approx 2{,}712.48$ Mpc, which we found above.

Overall, we must obvious conclude that the part of cosmology we are considering is essentially a science of averages.
In principle, this could be seen clearly from the beginning, if we retrospectively look a little more closely about the evaluation we carried out, e.g. the quasar catalog and the subsequent finding of R_{0a}.

Only the consideration of a large number of cosmic objects of the same kind results in the correct values of astrophysically and cosmologically relevant quantities, respectively, which then are partly mean values only.

7. Concluding remarks

The light path D(z) of the photons through the expanding universe corresponds to a dynamic distance and is therefore an apparent one. This distance is not identical to the today's distance $D_0(z)$ between the objects.
For every conceivable observer, the cosmic objects are not spatially where they appear at first glance!
In cosmology, nothing is what it seems to be if we look at big distances.

Of course, all cosmologically relevant astrophysical objects have a today's distance $D_0(z)$. However, this is not observable, but we can calculate it.
Photons emitted at this distance from the observed galaxy cannot have reached us so far.

A fundamental property of quantum mechanics is that it can only make probability statements about the microscopic objects it deals with. Here it is seen that both the measuring and the theorizing astrophysics and cosmology, respectively, strictly speaking, can only make statements about mean values of very distant and large numbers of objects.
This may be one of the reasons why both theories - the theory for the extremely small and the theory for the extremely large - do not fit together; i.e. cannot be merged together.

Note of thanks:
I would like to thank my wife Gudrun for the long-standing toleration and the corresponding endurance of my almost constant virtual absence. What would I be without her?!

8. Appendix

In this table appendix, we provide the essential data that we have used and some of the data that we have edited or generated for general purposes.

$< V >_i$	$< z >_i$	$\sigma_{m,i}$	$< V >_i$	$< z >_i$	$\sigma_{m,i}$	$< V >_i$	$< z >_i$	$\sigma_{m,i}$
17.12072194	0.269543711	1.25551062	19.5118161	1.28508799	0.79265674	19.7439932	1.86740102	0.8223715
18.42994924	0.434725324	0.69496662	19.4960406	1.30997857	0.82617985	19.7431839	1.90379949	0.8745066
18.77986464	0.514410603	0.68208433	19.5406994	1.33635871	0.79628275	19.73815	1.91629442	0.85608298
18.92177101	0.571495206	0.70268585	19.5648675	1.36044896	0.84936023	19.7370051	1.94113536	0.83013271
19.01993232	0.621120135	0.69571033	19.5526283	1.38646193	0.85285126	19.6390299	1.96661139	0.91303871
19.07454597	0.665043993	0.72385254	19.5667343	1.41249746	0.82510058	19.7247377	1.99498872	0.83486627
19.10685279	0.710045685	0.76943643	19.5917766	1.43823632	0.84883691	19.7073435	2.02761873	0.85770271
19.20756345	0.750830795	0.74776464	19.5835759	1.46348111	0.81435344	19.7225437	2.05895826	0.83582282
19.23878173	0.788362662	0.82397969	19.6146701	1.4877084	0.77561435	19.7209927	2.09067964	0.87548608
19.34673999	0.823077834	0.84208852	19.6560914	1.50872984	0.80798031	19.7166723	2.12286464	0.87190043
19.35605189	0.857111675	0.83026192	19.6421545	1.53039989	0.82193001	19.7562211	2.15726452	0.83914146
19.35379019	0.889902425	0.83562264	19.6730062	1.55031021	0.78502817	19.6955838	2.1915251	0.87311109
19.35354202	0.925268472	0.83309066	19.669718	1.57141117	0.81671189	19.7102256	2.23148844	0.89180926
19.36111675	0.958962211	0.80795962	19.691489	1.59370615	0.79783244	19.6203328	2.27565595	0.8814518
19.36687535	0.99085674	0.81407063	19.6689622	1.61663057	0.79869119	19.6516638	2.32895262	0.90747466
19.39208122	1.021072758	0.83447413	19.7130344	1.64024196	0.79496734	19.7034969	2.39616356	0.89952989
19.41216018	1.049862944	0.81581048	19.7208742	1.66227637	0.79948606	19.6915454	2.47184715	0.93743249
19.43737733	1.076128596	0.81828949	19.7568415	1.68460462	0.79535961	19.7660462	2.57089058	0.97654953
19.47736041	1.10186802	0.79353868	19.6973942	1.70912747	0.83259167	19.7708009	2.71401918	0.95905229
19.4307727	1.129618161	0.80360659	19.7453187	1.7323057	0.83488167	19.7781162	2.90122279	0.85728912
19.45345178	1.157690919	0.80262312	19.7723632	1.75403384	0.80160723	19.9208291	3.05796277	0.78948482
19.4499718	1.18469656	0.81310891	19.7568754	1.77625888	0.80788436	20.0279357	3.20401523	0.77347127
19.50609701	1.208890017	0.7810332	19.7599436	1.79742358	0.80969081	20.2283362	3.40521263	0.78550396
19.48940778	1.233098139	0.80906834	19.7587704	1.82113988	0.83363286	20.5549521	3.7254264	0.73269653
19.47597857	1.259028765	0.79685819	19.7435195	1.84394303	0.82211045	21.3169261	4.34427862	1.27303027

Table 7. Mean values from the quasar data set used according to [1].

$<z>_i$ (with i = 1, ..., 75) are the 75 mean values of the redshifts of the quasars in the redshift intervals formed.
$<V>_i$ are the associated 75 mean values of the apparent visual magnitude of the quasars.
$\sigma_{m,\ i}$ are the standard deviations with respect to the apparent magnitudes (m-axis in the redshift-magnitude diagram).

z_i (end of interval)	N_i	z_i (end of interval)	N_i
0.24669	622	3.45369	128,884
0.49338	3,891	3.70038	130,205
0.74008	12,827	3.94708	131,357
0.98677	25,495	4.19377	132,019

1.23346	41,724	4.44046	132,432
1.48015	58,818	4.68715	132,669
1.72685	78,456	4.93385	132,848
1.97354	97,109	5.18054	132,902
2.22023	110,358	5.42723	132,924
2.46692	117,810	5.67392	132,932
2.71362	121,463	5.92062	132,949
2.96031	123,820	6.16731	132,972
3.20700	126,835	6.41400	132,977

Table 8. Numbers N_i summed up in the redshift intervals z_i of the quasars according to [1].

SNIa	μ_{TRGB}	μ_{Ceph}	μ or $<\mu>$	m_{CSP_B0}	m_{SC_B}	m_B or $<m_B>$	M_i or $<M_i>$	V_{NED}	z
1980N	31.46		31.46	12.08		12.08	-19.38	1,306.00	0.004356347
1981B	30.96	30.91	**30.94**	11.64	11.62	**11.63**	**-19.31**	1,050.00	0.003502423
1981D	31.46		31.46	11.99		11.99	-19.47	1,306.00	0.004356347
1989B	30.22		30.22	11.16		11.16	-19.06	689.00	0.002298257
1990N		31.53	31.53	12.62	12.42	**12.52**	**-19.01**	1,050.00	0.003502423
1994D	31.00		31.00	11.76		11.76	-19.24	1,050.00	0.003502423
1994ae	32.27	32.07	**32.17**	12.94	12.92	**12.93**	**-19.24**	1,552.00	0.005176915
1995al	32.22	32.50	**32.36**	13.02	12.97	**13.00**	**-19.37**	1,886.00	0.006291019
1998aq		31.74	31.74	12.46	12.24	**12.35**	**-19.39**	1,368.00	0.004563157
1998bu	30.31		30.31	11.01		11.01	-19.30	689.00	0.002298257
2001el	31.32	31.31	**31.32**	12.30	12.20	**12.25**	**-19.07**	1,047.00	0.003492416
2002fk	32.50	32.52	**32.51**	13.33	13.20	**13.27**	**-19.25**	1,864.00	0.006217635
2003du		32.92	32.92	13.47	13.47	**13.47**	**-19.45**	2,422.00	0.008078922
2005cf		32.26	32.26	12.96	13.01	**12.99**	**-19.28**	2,244.00	0.007485178
2006dd	31.46		31.46	12.38		12.38	-19.08	1,306.00	0.004356347
2007af	31.82	31.79	**31.81**	12.72	12.70	**12.71**	**-19.10**	1,983.00	0.006614576
2007on	31.42		31.42	12.39		12.39	-19.03	1,306.00	0.004356347
2007sr	31.68	31.29	**31.49**	12.30	12.24	**12.27**	**-19.22**	1,702.00	0.005677261
2009ig		32.50	32.50	13.29	13.46	**13.38**	**-19.13**	2,534.00	0.008452514
2011by		31.59	31.59	12.63	12.49	**12.56**	**-19.03**	1,368.00	0.004563157
2011fe	29.08	29.14	**29.11**	9.82	9.75	**9.79**	**-19.33**	455.00	0.001517717
2011iv	31.42		31.42	12.03		12.03	-19.39	1,306.00	0.004356347
2012cg	31.00	31.08	**31.04**	11.72	11.55	**11.64**	**-19.41**	1,050.00	0.003502423
2012fr	31.36	31.31	**31.34**	12.09	11.92	**12.01**	**-19.33**	1,302.00	0.004343005
2012ht		31.91	31.91	12.66	12.70	**12.68**	**-19.23**	1,447.00	0.004826672
2013dy		31.50	31.50	12.23	12.31	**12.27**	**-19.23**	1,410.00	0.004703254

2015F		31.51	31.51	12.40	12.28	**12.34**	**-19.17**	1,271.00	0.0042396
						<M>=	**-19.24**		

Table 9. Summary of the data which we used from the 27 SNIa according to [3].

SNIa values that can be traced back to a mean value are marked in green (**bold**).
The individual meanings of the data can be found in the article mentioned.

The data for the angular-size redshift diagram can be found in full in [2].

References

[1] M.-P. Véron-Cetty and P. Véron, A Catalogue of Quasars and Active Nuclei, 13th edition, March 2010, http://www.obs-hp.fr/catalogues/veron2_13/veron2_13.html

[2] K. Nilsson, M. J. Valtonen, J. Kotilainen and T. Jaakkola, Astro. J. 413 (1993), 453.

[3] W. L. Freedman et al., The Carnegie-Chicago Hubble Program. VIII. An Independent Determination of the Hubble Constant Based on the Tip of the Red Giant Branch, arXiv.org:1907.05922

[4] The Planck Collaboration: Planck 2018 results. VI. Cosmological parameters, arXiv:1807.06209

[5] The Event Horizon Telescope Collaboration, The Astrophysical Journal Letters, 875:L1 (17pp), 2019 April 10, https://doi.org/10.3847/2041-8213/ab0ec7

[6] de.wikipedia.org/wiki/Messier_87, retrieved 18.12.2021

[7] de.wikipedia.org/wiki/Quasar, retrieved 18.12.2021

[8] de.wikipedia.org/wiki/UDFj-39546284, retrieved 18.12.2021

[9] G. Dautcourt, Was sind Quasare?, S. 68, Abb. 18, BSB B.G. Teubner Verlagsgesellschaft, 4. Auflage 1987

[10] A. Sandage, R. G. Kron, and M. S. Longair, The Deep Universe, Springer-Verlag, 1995, (Saas-Fee Advanced Course 23, Lecture Notes 1993, Swiss Society for Astrophysics and Astronomy, Publishers: B. Binggeli and R. Buser).

[11] E. M. Burbidge and G. Burbidge, chapter “The redshifts of galaxies and QSOs” in CURRENT ISSUES IN COSMOLOGY edited by Jean-Claude Pecker and Jayant Narlikar, © Cambridge University Press 2006

[12] St. Haase, New derivation of redshift distance without using power expansions, Fundamental Journal of Modern Physics, Volume 17, Issue 1, 2022, Pages 1-40
